SGG✧SGS  sc | nat  CrossMark

# A tectono-stratigraphic record of an extensional basin: the Lower Jurassic Ab-Haji Formation of east-central Iran

Mohammad Ali Salehi[1] · Reza Moussavi-Harami[2] · Asadollah Mahboubi[2] ·
Franz Theodor Fürsich[3] · Markus Wilmsen[4] · Christoph Heubeck[5]

**Abstract** The Lower Jurassic Ab-Haji Formation consists of siliciclastic strata which are widespread and superbly exposed across the Tabas and Lut blocks of east-central Iran. The formation records the geodynamic history of central Iran during the Early Jurassic in the aftermath of the main Cimmerian event (near the Triassic–Jurassic boundary) through its sedimentary facies and stratigraphic architecture and allows palaeogeographic and palaeoenvironmental reconstructions. We measured and studied three well-exposed outcrop sections and identified lithofacies and facies associations (fluvial plain, delta plain, delta front, prodelta, and shallow-marine siliciclastic shelf). The integration of all geological, stratigraphic, and sedimentological data shows a west-to-east continental-to-marine gradient within the Ab-Haji Formation. Based on thickness variations, lateral facies changes, palaeocurrent patterns, and changes in the nature of the basal contact of the Ab-Haji Formation on the Tabas and

Lut blocks, we locate the fault-bounded Yazd Block in the west and the Shotori Swell at the eastern edge of the Tabas Block as provenance regions. The pattern of thickness variations, rapid east–west facies changes, and provenance is best explained by a tectonic model invoking large tilted fault blocks in an extensional basin. The basal unit shows distinct increase in grain size at the base of the Ab-Haji Formation, similar to the Shemshak Group of the Alborz Mountains (the base of the Alasht Formation) and the non-marine time-equivalent succession of the Binalud Mountains of northeastern Iran. This grain size pattern may have been caused by rapid source area uplift due to slab break-off of the subducted Iran plate in the course of the Cimmerian collision in east-central Iran.

**Keywords** Early Jurassic · Cimmerian event · Facies association · Extensional basin · East-central Iran

✉ Mohammad Ali Salehi
 ma.salehi@sci.ui.ac.ir

1 Department of Geology, Faculty of Sciences, University of Isfahan, 81746−73441 Isfahan, Iran

2 Department of Geology, Faculty of Sciences, Ferdowsi University of Mashhad, 91775−1436 Mashhad, Iran

3 GeoZentrum Nordbayern, Fachgruppe PaläoUmwelt, Friedrich-Alexander-Universität Erlangen-Nürnberg, Loewenichstr. 28, 91054 Erlangen, Germany

4 Senckenberg Naturhistorische Sammlungen Dresden, Museum für Mineralogie und Geologie, Sektion Paläozoologie, Königsbrücker Landstr. 159, 01109 Dresden, Germany

5 Department of Geology, Universität Jena, Burgweg 11, 07749 Jena, Germany

## 1 Introduction

Within the Alpine–Himalayan–Indonesian mountain ranges, two distinct but largely superimposed orogenic systems exist: The older Cimmerian orogen, formed during the late Middle Triassic to the earliest Middle Jurassic, and the younger (Late Palaeocene to Late Eocene) Alpidian orogen, which together form the super-orogenic complex of the Tethysides (Sengör 1984). Both of these systems have been shown to include several sutures, with two dominant times of ocean closure along them (Sengör et al. 1988). These orogenic systems influenced relative sea-level changes and patterns of sedimentation during much of the Mesozoic and Cenozoic in the mentioned areas. The Cimmerian orogeny governed the Late Triassic–Jurassic sedimentation pattern of the composite Iran blocks,

Birkhäuser

including the Central-East Iranian Microcontinent (CEIM; Takin 1972; Wilmsen et al. 2009a, b). The CEIM consists of three large, fault-bounded, today north–south-oriented structural units: The Lut, Tabas, and Yazd blocks (Fig. 1a).
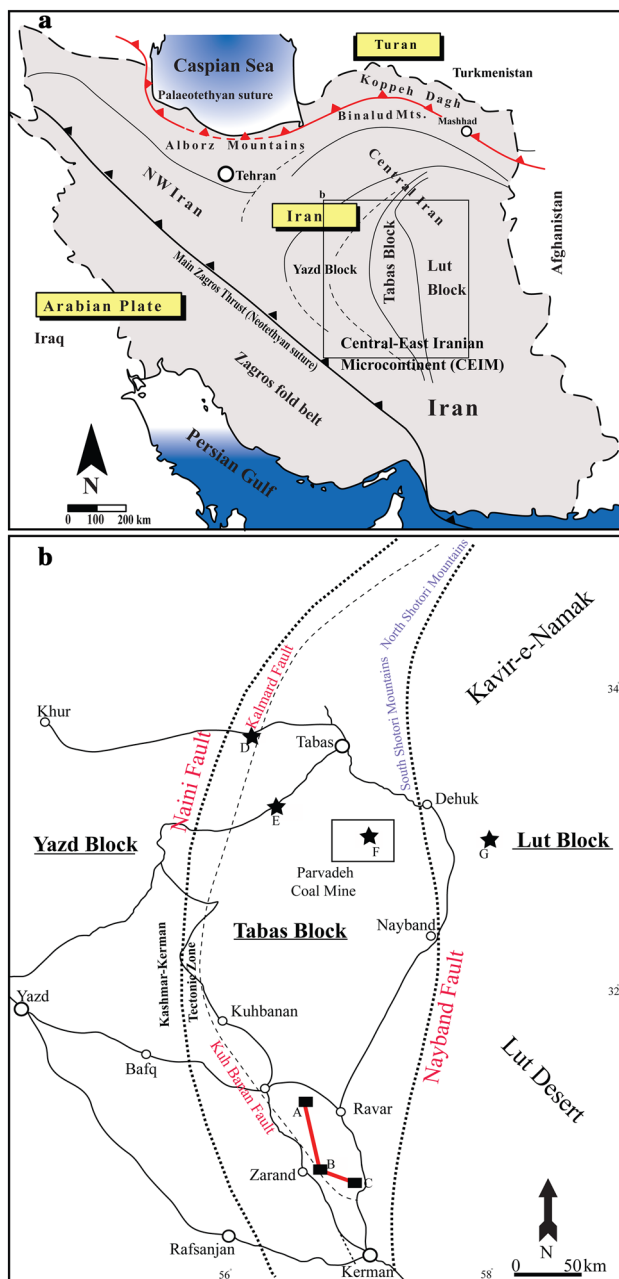


**Fig. 1 a** Structural and geographic framework of Iran showing the main sutures, structural units and geographic areas. **b** Locality map of east-central Iran with major structural units (blocks and block-bounding faults modified from Wilmsen et al. 2009a; Palaeotethys suture modified from Sengör et al. 1988). Previously measured sections are indicated by asterisks; new sections by rectangles. A. Ravar–Abkuh, B. Zarand–Chenaruyeh, C. Zarand–Eshkeli, D. Kuh-e-Rahdar, E. Simin-Sepahan, F. Parvadeh, G. Kuh-e-Shisui. The red line (A–B–C) marks the lithostratigraphic NW–SE cross section of Figs. 10 and 12

The Tabas and Yazd blocks are separated by a long, arcuate and structurally complex belt defined as the Kashmar–Kerman Tectonic Zone (KKTZ) (Haghipour and Pelissier 1977; Masoodi et al. 2013) (Fig. 1b) . The tectonic instability of the area is reflected in numerous sedimentologic and stratigraphic features (Fürsich et al. 2003, 2009a, b; Wilmsen et al. 2003, 2009a, b; Seyed-Emami et al. 2004a; Zamani-Pedram 2011).

During the Early Jurassic, the siliciclastic Ab-Haji Formation was deposited across two tilted fault blocks (Tabas and Yazd) of the CEIM (Wilmsen et al. 2009a, b; Salehi et al. 2014a, b). A detailed lithostratigraphic, lithofacies and provenance analysis of the Ab-Haji Formation suggested an Early Jurassic extensional tectonic setting for the three central-east Iranian blocks (Salehi et al. 2014a, b).

Among the three structural units of east-central Iran, the southern Tabas Block is a key area of this basin because it shows the thickest, most complete and best exposed sections of the Ab-Haji Formation within the region. In this study, we provide additional comprehensive descriptions of its stratigraphy and lithofacies to constrain the tectonic setting (Salehi et al. 2014a, b) and to better understand the Mesozoic geodynamic history of east-central Iran. This paper also aims to integrate available geologic, stratigraphic, and sedimentologic data (Salehi et al. 2014a, b) to correlate the Ab-Haji Formation with other regions of the Iran plate while considering its lateral facies and thickness changes, provenance, and tectonic controls.

## 2 Geological setting and palaeogeography

The study area is located on the southern Tabas Block in the central part of the CEIM (Takin 1972) which currently forms the central part of the Iran Plate (Fig. 1). This plate, an element of the Cimmerian microplate assemblage, became detached from Gondwana during the Permian and collided with the Turan Plate of Eurasia during the Late Triassic, thereby closing the Palaeotethys (Eo-Cimmerian event; e.g., Stöcklin 1974; Stampfli and Borel 2002; Horton et al. 2008; Fürsich et al. 2009a; Wilmsen et al. 2009a; Zanchi et al. 2016) (Fig. 2a). This Eo-Cimmerian Orogeny transformed the northern margin of the Iran Plate into an under-filled Carnian–Rhaetian flexural foreland basin (Wilmsen et al. 2009a). At the same time, Neotethys subduction started at its southwestern margin (e.g., Arvin et al. 2007). This process is inferred to have reduced the compression of the Iran Plate such that extensional basins formed which subsequently were filled with up to 3000 m of marine Norian–Rhaetian sediments (Nayband Formation of Central Iran; Fürsich et al. 2005a). New age dating results of eclogites, a metamorphic rock indicator of

**Fig. 2 a** Palaeogeographic and plate tectonic framework of the Middle East in the Early Jurassic (Middle Toarcian). The block boundaries of east-central Iran (Lut, Tabas and Yazd) are indicated by dashed lines in assumed Early Jurassic orientation (modified after Barrier and Vrielynck 2008). **b** Geodynamic model of Iran, not to scale, during the Hettangian–Pliensbachian (in the aftermath of the main-Cimmerian event; modified from Wilmsen et al. 2009b; Salehi et al. 2014a, b)
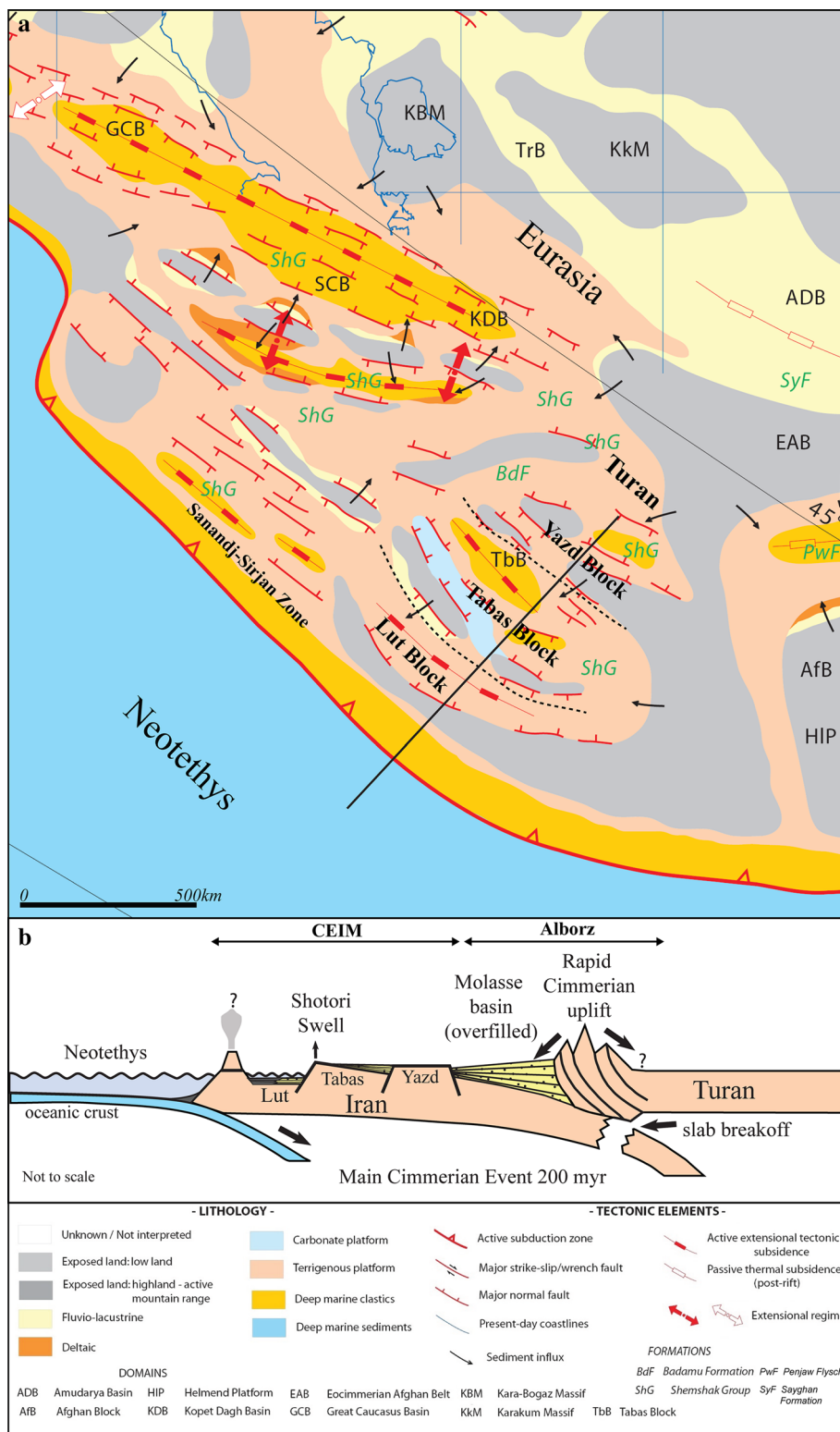


subduction zones, which have been found in the Sanandaj–Sirjan zone, indicate Neotethys Ocean subduction during the Early Jurassic (Davoudian et al. 2016). The main Cimmerian uplift and foreland deformation event occurred at the Triassic–Jurassic boundary, followed by a rapid denudation of the Cimmerian Mountains in northern Iran. This event also resulted in termination of marine sedimentation, followed by non-deposition or erosion, source-

area rejuvenation, and deposition of the Lower Jurassic Ab-Haji Formation in east-central Iran (Wilmsen et al. 2009b) (Fig. 2b). In addition, the complex tectonic regime of the southern Tabas Block influenced the Lower Jurassic sedimentation pattern.

Palaeogeographic reconstructions of the Early Jurassic (Thierry 2000) place the Iran Plate at the northern margin of the Neotethys at a palaeolatitude of ca. 40°–45°N (Fig. 2a). The distribution of marine and non-marine strata indicates that the Lut and some part of the Tabas blocks were mostly covered by the sea during the Early Jurassic whereas most of the Yazd Block remained emergent (Early Jurassic stratigraphic gap) (Fig. 2a–b).

According to several geodynamic models (e.g., Davoudzadeh et al. 1981, Soffel and Förster 1984; Soffel et al. 1996; Alavi et al. 1997; Besse et al. 1998), the CEIM experienced post-Triassic counterclockwise rotation around a vertical axis by 135° into its present-day position, associated with considerable lateral movements along the block-bounding faults (Fig. 1a). Rotation most probably took place in post-Jurassic times (Esmaeily et al. 2007; Bagheri and Stampfli 2008; Wilmsen et al. 2009a, 2015; Mattei et al. 2012, 2014, 2015) although both timing and amount of rotation (and its existence at all) have repeatedly been questioned (e.g., Muttoni et al. 2009a, b). However, Cifelli et al. (2013) demonstrated that the movements at the block-bounding fault between the Tabas and Lut blocks of the CEIM changed from extensional during the Jurassic to right-lateral transpressional during the Early Cretaceous to Palaeocene. Furthermore, Mattei et al. (2012, 2014, 2015) documented evidence of two distinct counterclockwise rotations phases of the CEIM during the Early Cretaceous and after the Middle–Late Miocene.

## 3 Regional stratigraphy

As elsewhere in Iran, there is a conspicuous change from Middle Triassic platform carbonates (Shotori Formation) to Norian–Bajocian siliciclastic rocks of the Shemshak Group of east-central Iran (Seyed-Emami 2003; Fürsich et al. 2005a, 2009a). This group is bordered by the Eo-Cimmerian unconformity at its base and by the Mid-Cimmerian unconformity at its top (Fig. 3). Fürsich et al. (2009a) provide detailed descriptions of the Upper Triassic–Middle Jurassic succession of the Shemshak Group in the Alborz Mountains in the context of the Cimmerian events while Wilmsen et al. (2009c) focused on the unit in northeastern Iran (Binalud Mountains near Mashad). On the Tabas Block, the Shemshak Group is less well studied. Fürsich

et al. (2005a) studied the Upper Triassic (Norian–Rhaetian) Nayband Formation; Toarcian–Lower Bajocian ammonites from the upper part of the Shemshak Group have been detailed by Seyed-Emami (1971) and Seyed-Emami et al. (1993, 2000, 2004b). The Ab-Haji Formation, however, has received little attention so far.

The Lower Jurassic Ab-Haji Formation crops out from the eastern margin of the Yazd Block throughout much of the Tabas Block, except at its eastern margin (Shotori Mountains), and continues onto the western Lut Block (Fig. 3). In the studied areas of the southern Tabas Block, the Ab-Haji Formation is well developed. It reaches a thickness of up to 700 m, but may be locally reduced to a few tens of meters towards the east. It mainly consists of thin- to thick-bedded greenish sand- and siltstones and locally contains thin coal seams. Over much of the Tabas Block, the basal contact is marked by coarse-grained quartzarenite described in more detail below. Its upper boundary is characterized by the appearance of calcareous strata of the Toarcian–Aalenian Badamu Formation. The rich ammonite fauna of this unit (e.g., Seyed-Emami 1971), in conjunction with the conspicuous Norian–Rhaetian fauna of the underlying Nayband Formation (Fürsich et al. 2005a), provide the biostratigraphic framework for the chronostratigraphic calibration of the Ab-Haji Formation.

## 4 Methods

We measured, described, and sampled three stratigraphic sections in the field (Fig. 1b, Table 1). All sections were logged bed-by-bed using a modified Jacob Staff (Sdzuy and Monninger 1985). Analysis of photo mosaics and field tracing of individual strata to document lateral and vertical stacking patterns as well as facies distribution supplemented the outcrop information.

Lithofacies were defined based on sedimentary structures and lithology. We established thirteen lithofacies types and five facies associations using the modified lithofacies classifications of Miall (1985, 2006) for facies analysis (Table 2). Facies associations were defined by stratal characteristics or by groups of genetically related sets of strata, grain size, constituent lithofacies as well as vertical and lateral relationships. This allowed the interpretation of depositional settings and provided input data for a reconstruction of the palaeogeography of east-central Iran during the Early Jurassic. Palaeocurrent indicators were recorded at 25 locations to constrain sediment dispersal patterns.
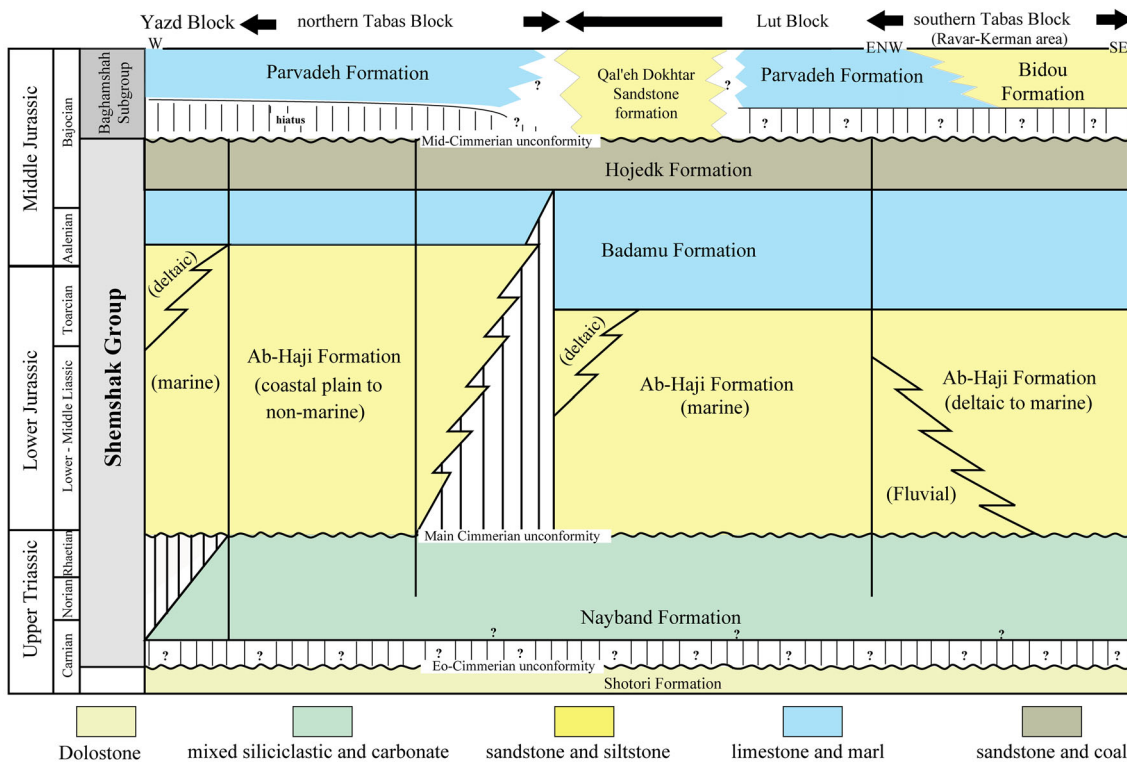
**Fig. 3** Lithostratigraphic framework of the Upper Triassic to Lower Middle Jurassic strata of the northern and southern Tabas Block and the western Lut Block, east-central Iran (modified from Wilmsen et al. 2009a; Salehi et al. 2014b)

## 5 Sections

The measured sections allow to construct a stratigraphic cross-section trending southeast–northwest through the southern Tabas Block (Fig. 1b, Table 1). These sections are embraced by the Kuh Banan Fault (a branch of Naini Fault) in the southwest and the Nayband Fault in the east (Fig. 1a). The general structure of the area is a large syncline with a NW–SE trend, also termed "Zarand Trough" by Huckriede et al. (1962) or "Kerman coaly syncline" (Fig. 4). The region is affected by the structural grain consisting of along-strike faults, short faults and lineaments which are typical structural elements in the region (Hashmie et al. 2016). The three sections are described below and are illustrated in detail in Figs. 5 and 6.

### 5.1 Ravar–Abkuh (Fig. 6a)

This section (∼684 m thick) was measured at Abkuh valley, about 15 km west of Ravar (Fig. 4). The base of the Ab-Haji Formation is characterized by a distinct increase in grain size within a coarsening-upward succession that overlies the top of the marine, fine-grained siliciclastic rocks of the Nayband Formation (at 230 m, Figs. 5a, 6a). The basal 120 m consists of coarsening-upward, thick-bedded, large-scale trough-cross-bedded sandstone with minor interbedded siltstone and shale (Fig. 5a). These are overlain by ∼110 m of red, plant-debris-bearing, interbedded shale and fine-grained siltstone. Up-section, fining-upward, trough cross-bedded sandstone commonly contains plant material, large tree trunks and root traces within the finer-grained rocks. The upper 234 m of the formation generally consist of laminated green shale with two interbedded coarsening-upward sandstone packages.

**Table 1** Measured sections in the Ravar and Zarand area, Southern Tabas Block, east Central Iran

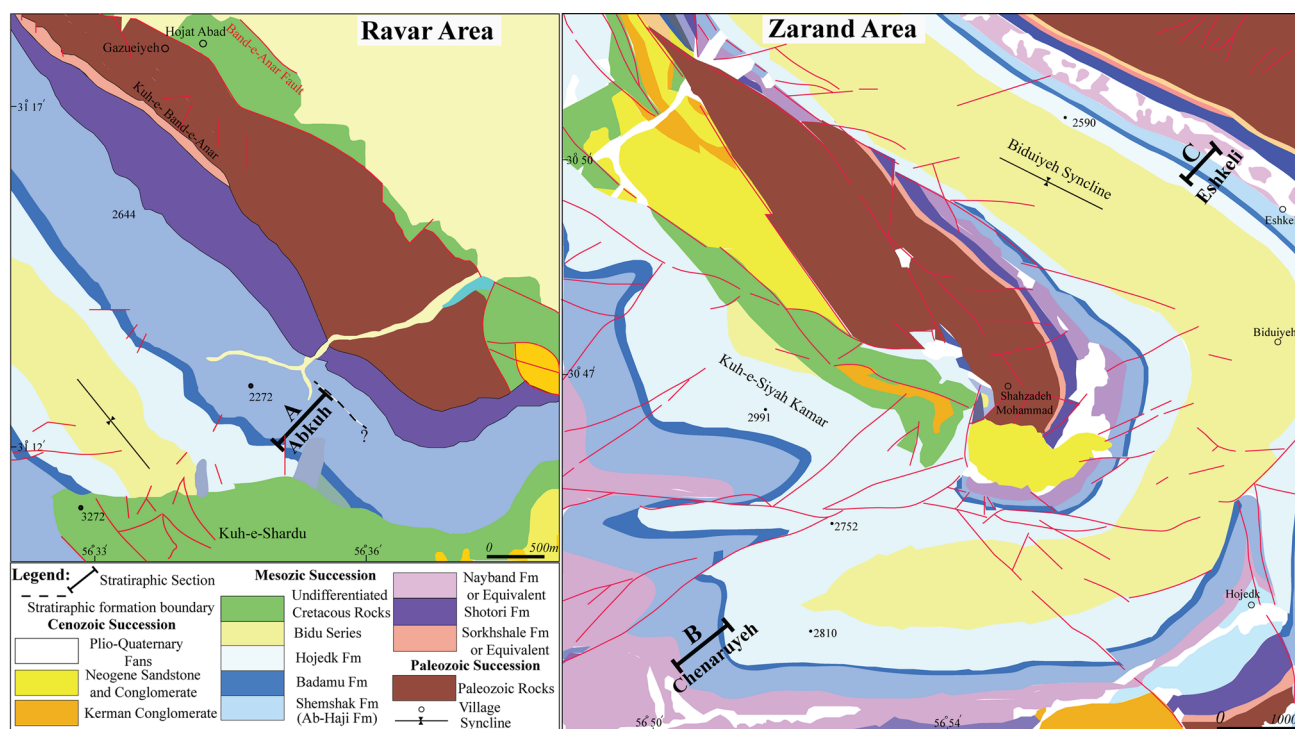|   | Location | Co-ordinates | Measured thickness (m) |
|---|----------|--------------|------------------------|
| 1 | Abkuh valley, 15 km west of Ravar | N31°14′31″ E56°35′00″ | 684 |
| 2 | Chenaruyeh valley, 25 km northeast of Zarand | N30°44′30″ E56°51′18″ | 702 |
| 3 | Eshkeli Coal Mine, 35 km northeast of Zarand | N30°49′34″ E57°00′42″ | 402 |

**Fig. 4** Geological map of the study area simplified from the geological maps of Ravar and Zarand in the scale of 1:100.000 (Geological Survey of Iran 1995a, b). Locations of measured stratigraphic sections are shown. The boundary between the Ab-Haji and Nayband formations in the Ravar geological map is based on our fieldwork and the subdivision of the hitherto undifferentiated "Shemshak Formation"

The Ab-Haji Formation at this locality is overlain by fossil-rich (ammonite- and belemnite-bearing) limestone and green marl of the Badamu Formation (Fig. 5b).

## 5.2 Zarand–Chenaruyeh (Fig. 6b)

The section (~702 m in thickness) was measured at Chenaruyeh valley, 25 km northeast of Zarand (Fig. 4). The base of the Ab-Haji Formation is sharp and erosional (Fig. 5c) and lies within a coarsening-upward sequence similar in architecture to the Ravar–Abkuh section (at 418 m, Fig. 6b). The basal 70 m constitute a coarsening-upward succession of medium- to coarse-grained sandstone with interbedded, thin, clast-supported conglomerate. This unit is capped by 140 m of laminated green shale, followed by 170 m of fine- to medium-grained sandstone interbedded with shale and fine-grained siltstone, stacked into several coarsening-upward packages. The sandstone bears plant debris; its bedding planes are rippled. The remaining section consists of 275 m of laminated green shale with two packages of coarsening-upward, trough-cross-bedded, weakly bioturbated sandstone. The overlying Badamu Formation is composed of fossiliferous limestone and marl, including ammonites and bivalves.

## 5.3 Zarand–Eshkeli (Fig. 6c)

The Zarand–Eshkeli section of the Ab-Haji Formation (402 m) was measured at the Eshkeli Coal Mine, 35 km northeast of Zarand (Figs. 4, 5d). The contact between the Ab-Haji and Nayband Formations is similar to that of Ravar–Abkuh and Zarand–Chenaruyeh sections (at 78 m, Figs. 5d, 6c). The Ab-Haji Formation starts with 15 m of trough-cross-bedded, fine- to medium-grained, coarsening-upward sandstone. This unit is followed by 60 m of laminated, green shale, which grades upwards into a 70-m-thick package consisting of three coarsening-upward sandstone units with abundant plant debris and ripple surfaces. A slump structure was recorded at 160 m (Fig. 6c). The remaining thickness is composed of interbedded thin sandstones and shale. Hummocky cross-stratification and intensive bioturbation is common. The Ab-Haji Formation ends with a 65 m-thick succession of laminated shale. The contact to the overlying Badamu Formation is sharp. The base of this formation is represented by a belemnite-rich limestone.
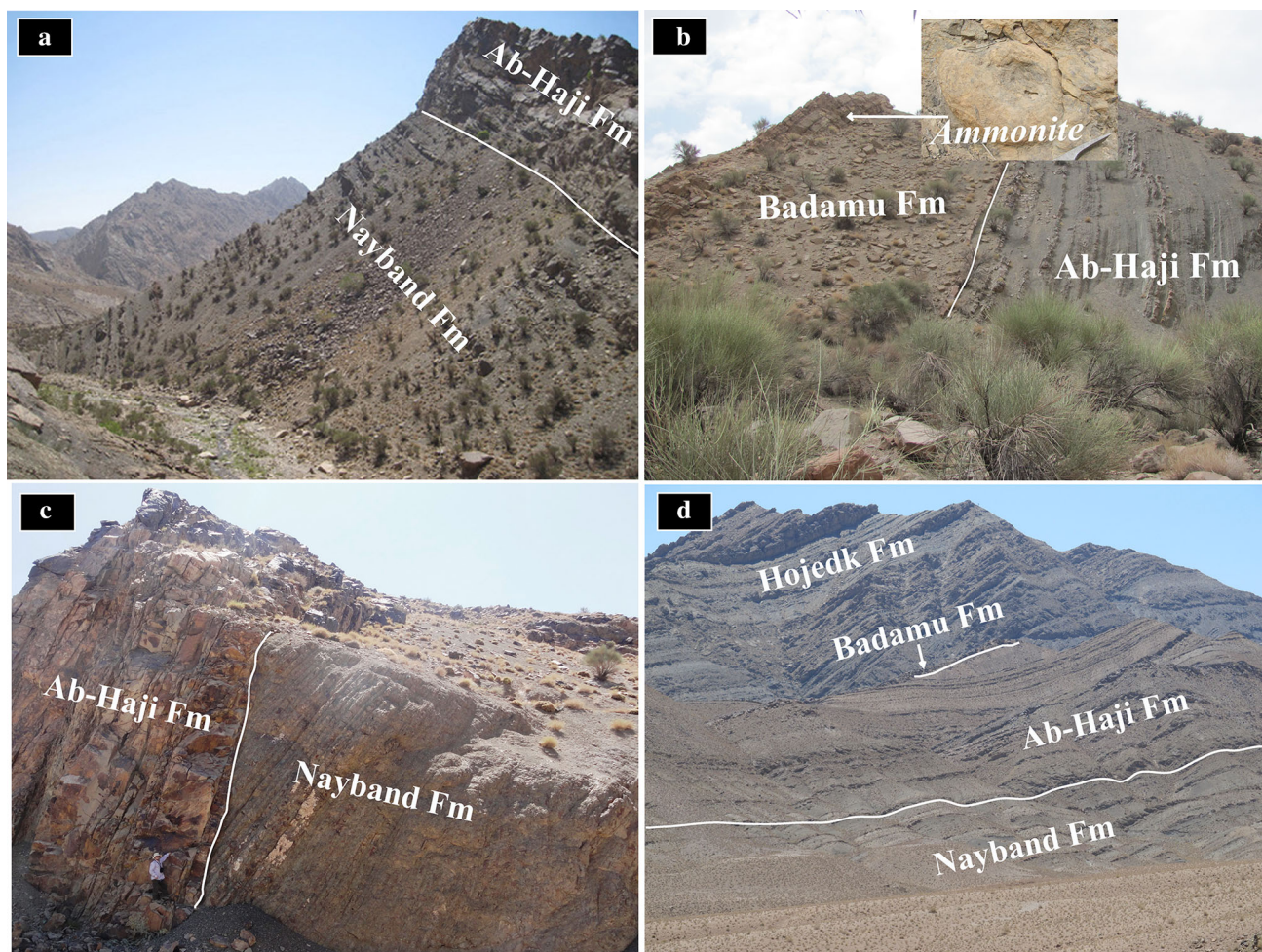
**Fig. 5** Overview field photographs of the Ab-Haji Formation in east-central Iran. **a** Overview of the Ravar–Abkuh section; view to the east from the top of the Upper Triassic Nayband to the Lower Jurassic Ab-Haji formations; note the conspicuous increase in slope angle at the formational contact caused by a distinct increase in grain size and weathering resistance. **b** Interbedded siltstones and shales of the uppermost part of the Ab-Haji Formation are overlain by the ammonite-rich marls and limestones of Badamu Formation (Ravar–Abkuh section). View is to the west. **c** Sharp, erosional contact of the fine-grained siltstones and sandstones of the Nayband Formation and coarse-grained sandstones of the Ab-Haji Formation (Zarand–Chenaruyeh section). View to the east. **d** Overview of the Zarand–Eshkeli section; view to the south from the top of the Upper Triassic Nayband to the Lower Jurassic Ab-Haji formations. At the top, fluvial, coal-bearing strata of the Hojedk Formation are underlain by limestones and marls of the Badamu Formation

# 6 Lithofacies, facies associations and depositional environments

## 6.1 Lithofacies

On the basis of lithology, sedimentary structures and textures as well as bed geometry, thirteen lithofacies were identified in the field (lithofacies codes modified after Miall 1985, 2006). Lithofacies analysis distinguish two coarse-grained (Gcm, Gt), seven medium-grained (St, Se, Sp, Sr, Sh, Shc, Sl), three fine-grained (Fl, Fm, Fc), one interbedded sandstone-claystone (Sr/Fl) and one coal lithofacies (C) (Figs. 7, 8, 9). A similar set of lithofacies was also recognized and described within the Ab-Haji Formation of the northern Tabas Block by Salehi et al. (2014a). Thus, the main information and details on lithofacies have been condensed into Table 2 and Figs. 7, 8, 9.

## 6.2 Facies associations and depositional environments

Based on stratigraphic lithofacies trends and spatial associations, we identified five major facies associations, representing fluvial channels with associated flood plain and swamps, delta plain, delta front, prodelta and shallow-marine siliciclastic shelf depositional environments within the Ab-Haji Formation. Similarily, these facies associations also occur on the northern Tabas Block (Salehi et al. 2014a) and their description is consequently kept short here. Each facies association consists of a number of
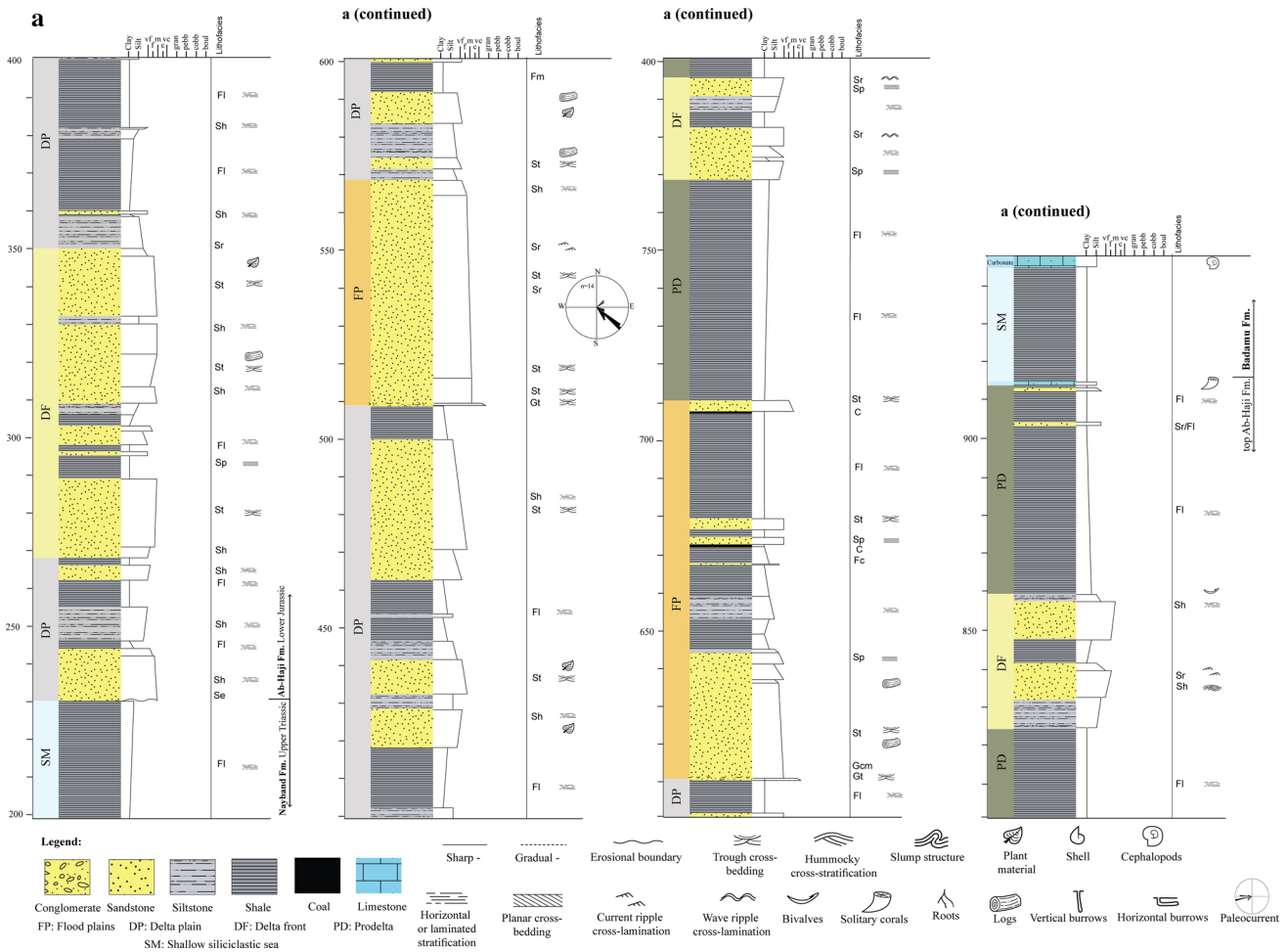
**Fig. 6** Stratigraphic logs of the Ab-Haji Formation. **a** Ravar–Abkuh section. **b** Zarand–Chenaruyeh section. **c** Zarand–Eshkeli section. For color code see Fig. 12. Grain-size code: *vf* very fine-, *f* fine-, *m* medium-, *c* coarse-, *vc* very coarse-grained sandstone

lithofacies characteristic of specific sub-environments (Table 2); Figs. 7, 8, 9 show typical facies associations from the southern Tabas Block. The stratigraphic distribution of the five major facies associations in the study area is shown in representative logs in Fig. 10.

### 6.2.1 Fluvial plains

*Description*: This facies association includes channels, floodplains and swamps sub-associations. Channel deposits include lenticular to more rarely tabular, fining-upward conglomerates (Gcm, Gt) and sandstones (St, Se, Sr) (Fig. 7a–b). The large-scale trough cross-bedded sandstone bodies fines upward into green to grey argillaceous siltstone or siltstone (Fl, Fm) of floodplain origin, and parallel-laminated or ripple-bedded fine-grained sandstone beds (Sh, Sr), bearing plant debris and coalified wood fragments (Fig. 8a). The fine-grained sandstone and siltstone beds occasionally display current ripples (Fig. 7c). Strata of this facies are well developed at Ravar–Abkuh. Swamp facies

are dominated by fine-grained siliciclastic rocks such as dark-grey laminated siltstone, carbonaceous claystone (Fc) and coaly shale (C) (Fig. 7e).

*Interpretation*: The complex, mostly lenticular sandstone beds, occasionally exhibiting lateral migration, likely represent channel deposits of low-sinuosity rivers (e.g. Collinson 1996; Veiga et al. 2002) that drained the adjacent exposed area. Fluvial channels occur in the southern Tabas Block, in the Ravar–Abkuh section. Palaeocurrent analyses of fluvial channels in this section show unimodal patterns with a very low spread in flow direction to the southeast (Fig. 6a). Deposition of greenish-grey, unfossiliferous siltstone and argillaceous siltstone took place in interchannel floodplains. Sand was likely deposited by crevasse splays during flooding (e.g. Farrell 1987). Like at Ravar–Abkuh section, where coal beds and carbonaceous clay- and siltstones occur associated with other fluvial sub-environments, they probably formed in swampy areas of vegetated flood plains (e.g. McCabe 1987).
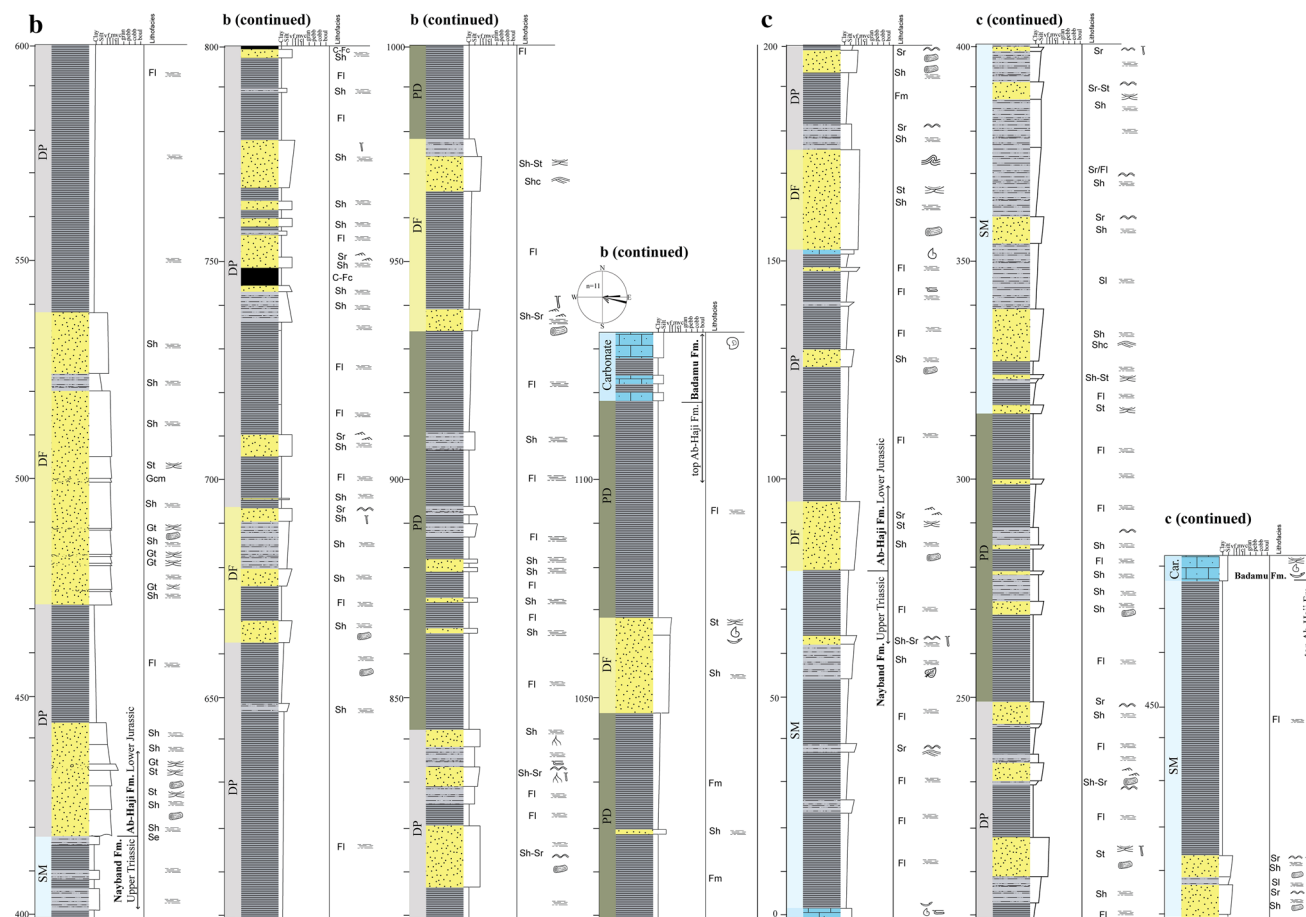
**Fig. 6** continued

### 6.2.2 Delta plain

*Description*: This facies association is composed of thick coarse- to fine-grained sandstone, ripple-laminated silt-stone, highly carbonaceous shale, interbedded red to gray claystone (Fl, Fm) and coal seams (C) (Fig. 8b). The facies association varies in thickness from 20 to 50 m and shows a fining- and thinning-upward trend. Trough and planar cross-stratified sandstone beds (St, Sp) show lenticular to sheet-like geometry. Wood fragments are abundant, and tree logs occur disorderedly at the base of some sandstone units (Fig. 8c).

*Interpretation*: This facies association characterizes environments that oscillate between fluvial and deltaic settings. Thick siltstone and fine-grained sandstone beds commonly associated with red and carbonaceous shale indicate deposition on the plain of a fluvial-dominated delta. The thick package of fine-grained siliciclastic rocks of this facies association is interpreted as representing various delta-plain sub-environments such as small distributaries and swamps which were filled with sediment deposited during successive flood events (Coleman 1988). The recent

discovery of dinosaur footprints reported by Kellner et al. (2012) from the Ab-Haji Formation of the southern Tabas Block supports the delta-plain-origin of this facies association. Their placement within a deltaic system is also based on their close association with strata representing delta front environments (e.g., Ravar–Abkuh section at 350–510 m).

### 6.2.3 Delta front

*Description*: Characteristic features of delta fronts are sequences that coarsen upward from fine- to medium- or to coarse-grained sandstone. The sandstones are nearly invariably large-scale trough cross-bedded (St) or horizontally laminated (Sh) and occasionally slump-folded; they contain plant debris and wood fragments with wave and current ripples (Sr) (Figs. 7d, 8e). At the top of the thickening-upward-cycles, immature microconglomerates to conglomerates (Gcm, Gt) containing wood fragments occur (e.g., Zarand–Chenaruyeh section at 470–500 m). The coarsening-upward sandstone packages show a clear stacking pattern at the western margin of the southern
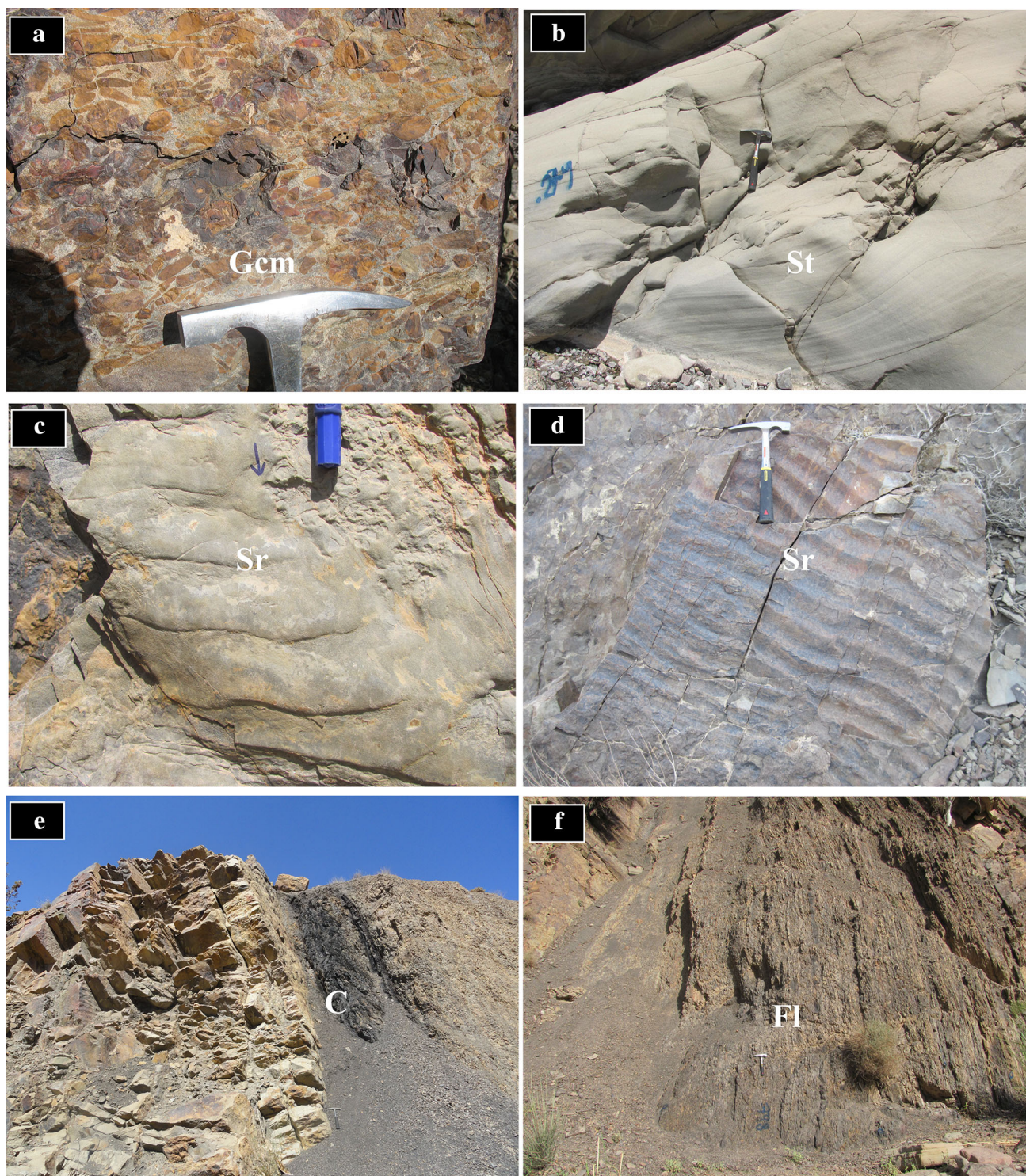
Fig. 7 Representative lithofacies of the Ab-Haji Formation. **a** Gcm lithofacies. **b** Trough cross-bedded sandstone lithofacies (St). **c** Sr lithofacies with current-rippled sandstone. **d** Sr lithofacies with wave-rippled sandstone. **e** Coal (C) lithofacies. **f** Beds of laminated siltstone and mudstone; (Fl) lithofacies. These lithofacies are interpreted as representing deposition in a variety of environments from continental to shallow-marine siliciclastic shelf

Tabas Block. At Ravar–Abkuh, a large-scale cross-bedded, medium- to coarse-grained sandstone overlies a thick coarsening-upward sequence (Fig. 8d).

*Interpretation*: The systematic changes in grain size, bed thicknesses, and sedimentary structures are characteristic of delta-front deposits (Wright 1985; Elliott 1986;
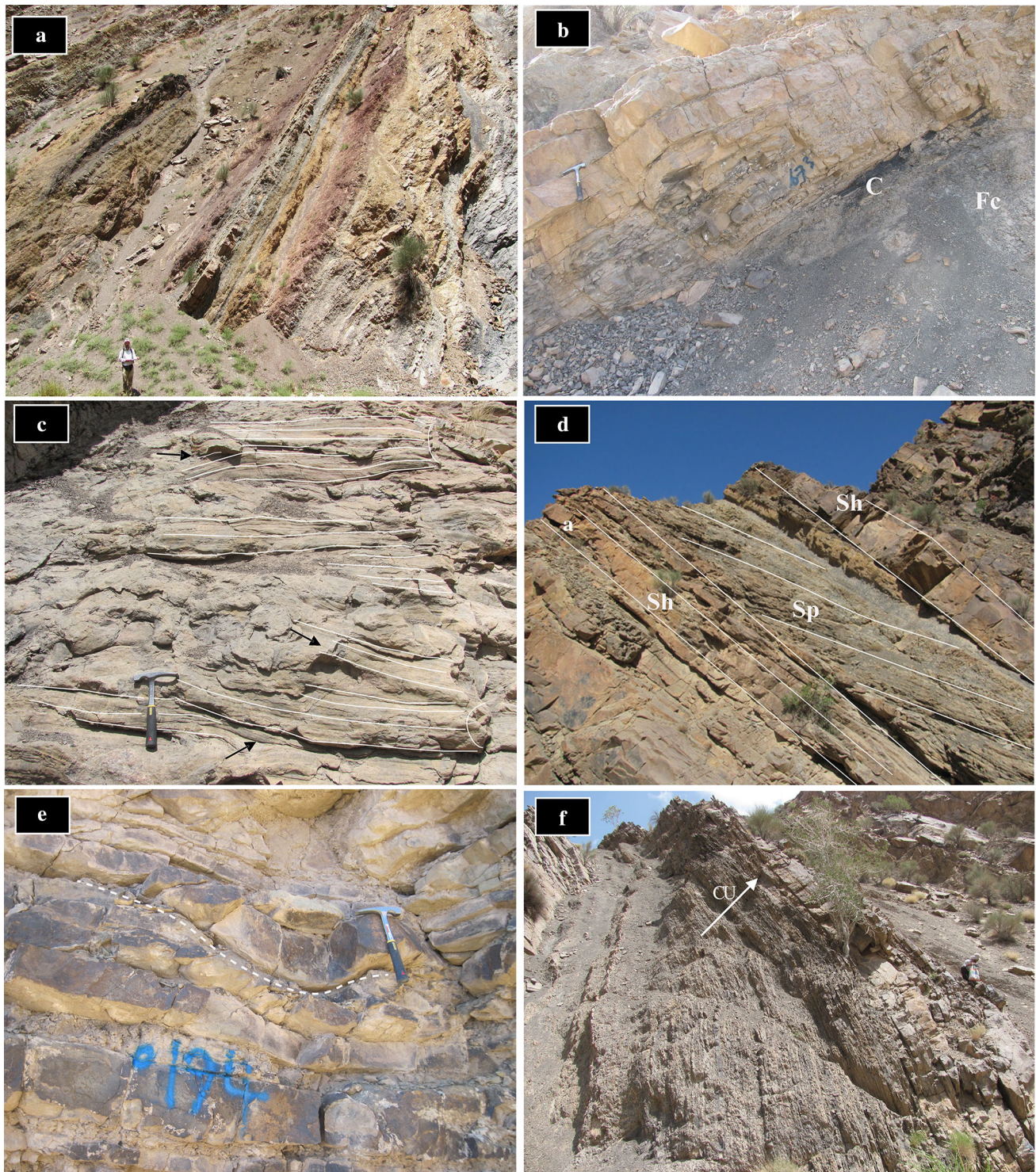
**Fig. 8** Field aspects and facies associations of the Ab-Haji Formation. **a** The red and gray siltstones and shales between sandstones formed in a continental setting (fluvial plain facies association) (Ravar–Abkuh section); view to the northeast. **b** Carbonaceous claystone (Fc), coal (C) and siltstone to fine-grained sandstone of the flood-plain swamp facies within the fluvial-plain facies association (Ravar–Abkuh section). **c** Sandstone casts of large tree trunks (outlined) in the delta-plain facies association (Ravar–Abkuh section). **d** Large-scale cross-bedded sandstones of the upper-delta-front facies overlie a thick coarsening-upward lower-delta-front facies (delta front facies association, Ravar–Abkuh section). **e** Small slump-fold above undisturbed bedding in delta-front sandstones (Zarand–Eshkeli section). **f** Coarsening-upward (CU) delta-front sandstones of the Ab-Haji Formation (Ravar–Abkuh section)
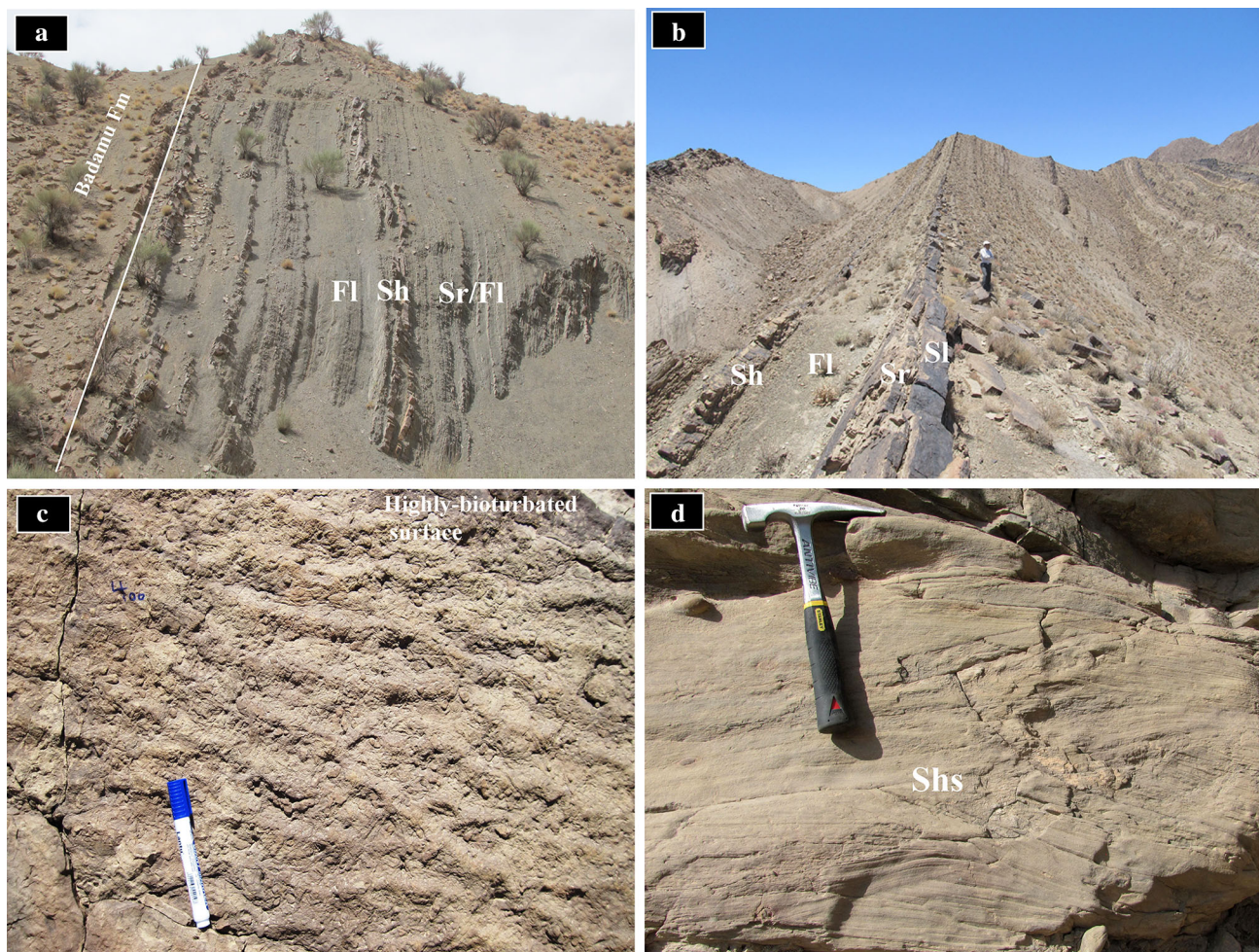
Fig. 9 Field aspects and facies associations of the Ab-Haji Formation. **a** Dark green to gray shales interbedded with siltstone and fine-grained sandstone of the prodelta facies association grade upsection (towards the left) into brown limestones and marls of the open marine Badamu Formation (Ravar–Abkuh section). **b** Shallow-marine facies association, characterized by well-bedded, horizontal to very-low-angle cross-stratified sandstone and siltstone (Zarand–Eshkeli section). **c** Highly bioturbated rippled surface on fine-grained sandstone of the shallow-marine facies association (Zarand–Eshkeli section). **d** Hummocky cross-stratified sandstone of the shallow-marine facies association (Ravar–Abkuh section)

Bhattacharya 2006). The thickening- and coarsening-upward cycles can be interpreted as shallowing cycles within a deltaic system. Several slumped beds indicate a depositional slope and sediment instability, probably related to high sedimentation rates or oversteepening (García-García et al. 2011). The general stacking pattern in thickening-upward packages reflects periodic progradation of delta fronts by strong variations in sediment supply, possibly due to changes in tectonic activity.

### 6.2.4 Prodelta

*Description*: The facies association consists of laminated shale (Fl) and alternations of cross-laminated siltstone and fine-grained sandstones (Sr/Fl), the latter being bioturbated and containing abundant plant debris, wood fragments, and occasionally marine fossils (Fig. 9a). Commonly, these sediments are organized in coarsening-upward sequences and grade into overlying delta-front sandstones (Fig. 8f).

*Interpretation*: Based on their lithological characters and their close association with delta-front sandstones, this facies association is interpreted as representing a prodelta setting of low to intermediate energy (e.g., Wright 1985). The sandstone–argillaceous siltstone and shale alternations record deposition by density currents and can be interpreted as prodelta turbidites (Coleman and Prior 1982; Leren et al. 2010), which in the case of the upper part of the Ravar–Abkuh and Zarand–Chenaruyeh sections deepen-and fine-upwards into deeper marine offshore shelf carbonates of the Badamu Formation. Prodelta sediments are well developed at the western margin of the southern Tabas Block.

**Table 2** Description and interpretation of sedimentary facies (lithofacies codes modified after Miall 1985, 2006; supplemented and modified after Salehi et al. 2014a)

| | Facie code | Characteristic | Petrofacies | Sedimentary processes; environmental interpretation | Occurrence |
|---|---|---|---|---|---|
| 1 | Gcm | Clast-supported polymictic conglomerates, pebble to granule with rare boulder grain-size, low roundness (subangular) and sphericity, very poor sorting, immature conglomerate, with reddish brown sandy matrix, common clast includes sedimentary rocks (red sandstone or siltstone and milky chert), massive or crudely stratified, marked by erosional and sharp base and upper contact is usually gradational with Sh and St, thickness ranging from 0.5 to1 m | Polymictic conglomerates | Deposition by rapidly waning flow regime, with sediment transport occurring via traction currents and marked by high sediment supply from the land. Deposition in fluvial channels | Sections A–B (Fig. 7a) |
| 2 | St | Trough cross-bedded sandstone, medium—to coarse-grained sand, rounded and high sphericity, good sorting, mature sandstone, set thickness generally 3–5 m, lenticular or wedge-shaped bodies, gradational with facies Gt and is erosional with facies Fm | Litharenite (chertarenite, phyllarenite, sedarenite) | Deposited as dunes or bars in response to unidirectional currents (e.g. Miall 2006); Deposition in fluvial channel; delta plain and front; upper shoreface | Sections A–C (Fig. 7b) |
| 3 | Se | Erosional scours with intraclasts, medium—to coarse-grained sand sometimes pebbly at base, solitary or grouped sets; set thickness generally 5–20 cm, associated with St | Litharenite (chertarenite, phyllarenite, sedarenite) | Dunes and scour fills in fluvial and delta plain | Sections A–B |
| 4 | Sp | Planar cross-bedded sandstone, fine—to medium-grained sand, sub-rounded and low sphericity, moderate sorting, sub-mature sandstone, set thickness generally 0.5–1 m, white, gray to yellowish brown, lenticular to tabular geometry, with erosional base and comonly grading to facies (Sh) | Litharenite (chertarenite, phyllarenite, sedarenite) | Migration of 2D dunes in response to unidirectional currents on fluvial bedforms, mostly close to river banks (Harms et al. 1975); also deposition in shoreface of a shallow marine siliciclastic shelf | Section A (Fig. 8d) |
| 5 | Sr | Current and sometimes wave-rippled, cross-laminated sandstone, very fine—to medium-grained sand, well-rounded with high sphericity, well sorted grains, mature to super-mature sandstone, thin sheets-like geometry, set thickness generally 0.1–0.3 m, associated with Sh and Fl | Sublitharenite to chertarenite | Deposition under subaqueous traction conditions by low flow regime (Harms et al. 1975); current ripple in fluvial flood plains and wavy ripple in upper shoreface | Sections A–C (Fig. 7c, d) |
| 6 | Sh | Horizontally laminated sandstone, fine—to coarse grained sand, sheet or tabular, well-rounded and high sphericity, well sorted graing, mature sandstone, set thickness generally 1–5 m, lower contact is gradational with facies St and its upper contact is with facies Sr, Fl and Fm | Litharenite (chertarenite, phyllarenite, sedarenite) | Deposited under the condition of either upper or lower flow regime by unidirectional currents (Miall 2006); on shallow marine siliciclastic shelf | Sections A–C (Figs. 7e, 8b) |
| 7 | Shc | Hummocky cross-bedded sandstone, fine—to medium-grained sand, well-rounded with high sphericity, well sorted grains, mature to super-mature sandstone, set thickness 0.1–0.3 m, associated with Sl | Litharenite (chertarenite, phyllarenite, sedarenite) | Oscillatory and/or combined flow deposits produced by storm on shallow marine siliciclastic shelf (e.g. Myrow and Southard 1996) | Section C (Fig. 9d) |

**Table 2** continued

| | Facie code | Characteristic | Petrofacies | Sedimentary processes; environmental interpretation | Occurrence |
|---|---|---|---|---|---|
| 8 | Sl | Low-angle (<10°) cross-bedded sandstone, fine—to medium-grained sand, well-rounded with high sphericity, well sorted grains, mature to super-mature sandstone, large wedge-shaped sets; set thickness 0.2–1 m, associated with Shc and Sr | Litharenite (chertarenite, phyllarenite, sedarenite) | Accretionary migration of 2D and 3D dunes in response to unidirectional currents in lower to upper flow regime transition (Cant and Walker 1976); oscillation of wave on shallow marine siliciclastic shelf | Section C (Fig. 9b) |
| 9 | Fl | Horizontally laminated claystone and siltstone, light green to gray with little organic matter, clay and silt size, plant fossil debris, sheet-like bodies, set thickness generally 10–20 m, gradational contact with facies Sh or Sr in lower part and with facies Fm in upper part | Siltstone; claystone | Deposition from suspension across low relief, abandoned flood plains and/or deposition in distal part of prodelta (e.g. Wright 1985) | Sections A–C (Figs. 7f, 9a) |
| 10 | Fm | Massive claystone to siltstone, clay size, gray to green colours with little organic matter, set thickness generally 5–25 m, lower contact is typically gradational, whereas the upper contact is usually sharply truncated | Siltstone; claystone | Suspension deposition with little or no current activity in overbank settings or abandoned channel in fluvial and delta plains (Miall 1985) | Section B (Fig. 8a) |
| 11 | Fc | Weakly horizontally laminated carbonaceous claystone to siltstone, clay size, black to dark gray colour with high organic content, wood and plant debris, set thickness generally 5–10 m, associated with Fl, C and Sr/Fl | Siltstone; claystone | Deposition from suspension in vegetated coastal swamp or flood plain | Sections A — B (Fig. 8b) |
| 12 | Sr/Fl | Interbedded rippled sandstones and mudstones, with wavy bedding and planar laminations, plant debris, set thickness generally 5–10 cm, associated with Fm and C | Sublitharenite–siltstone | Alternating strong and weak flows in coastal plain and inner shelf setting | Sections A, C (Fig. 9a) |
| 13 | C | Carbonaceous claystone grading to coal, clay and silt size, plant debris, set thickness generally 0.3–0.9 m, lower contact of this facies is ussally gradational with Fm and upper contact is erosional with facies St | Coal | Deposited most likely in vegetated depressions on coastal swamp or flood plain under clastic-sediment starvation condition (e.g. McCabe 1987) | Sections A–B (Fig. 8b) |

### 6.2.5 Shallow-marine siliciclastic shelf

*Description*: Horizontally to very-low-angle cross-stratified sandstone (Sh, Sl), ranging in thickness from 0.5 to more than 1 m, are occasionally interbedded with siltstones and shales (Fl, Sr/Fl) (e.g., Zarand–Eshkeli section at 320 m) (Fig. 9b). The sandstones are topped by ripple surfaces (Sr) and commonly exhibit bioturbation (e.g., Zarand–Eshkeli section at 400 m) (Fig. 9c). Hummocky cross-stratification (Shc) was encountered in the Zarand–Eshkeli section (Fig. 9d).

*Interpretation*: The sandstone units represent several sub-environments on a shallow-marine siliciclastic shelf. Large-scale low-angle cross-bedded sandstone, commonly coarsening-upward, is interpreted as shoreface sequence (e.g., Reineck and Singh 1973). Hummocky cross-stratification in combination with horizontal lamination and oscillation ripples indicates deposition by combined flows, produced by storm-generated waves (Myrow and Southard 1996). The association of hummocky cross-stratification with shoreface sequences also demonstrates the shallow-water origin of the structure which otherwise also may form in greater water depths by internal waves propagating along the pycnocline and breaking onto the shelf (Morsilli and Pomar 2012).

## 7 Discussion

A reconstruction of the palaeogeography of the CEIM during the Early Jurassic requires detailed knowledge of the spatial and temporal distribution of the facies of the Ab-Haji Formation. In the following, we thus discuss its correlation with other parts of the Iran plate, its lateral facies and thickness changes, its provenance, and the tectonic controls on its deposition.
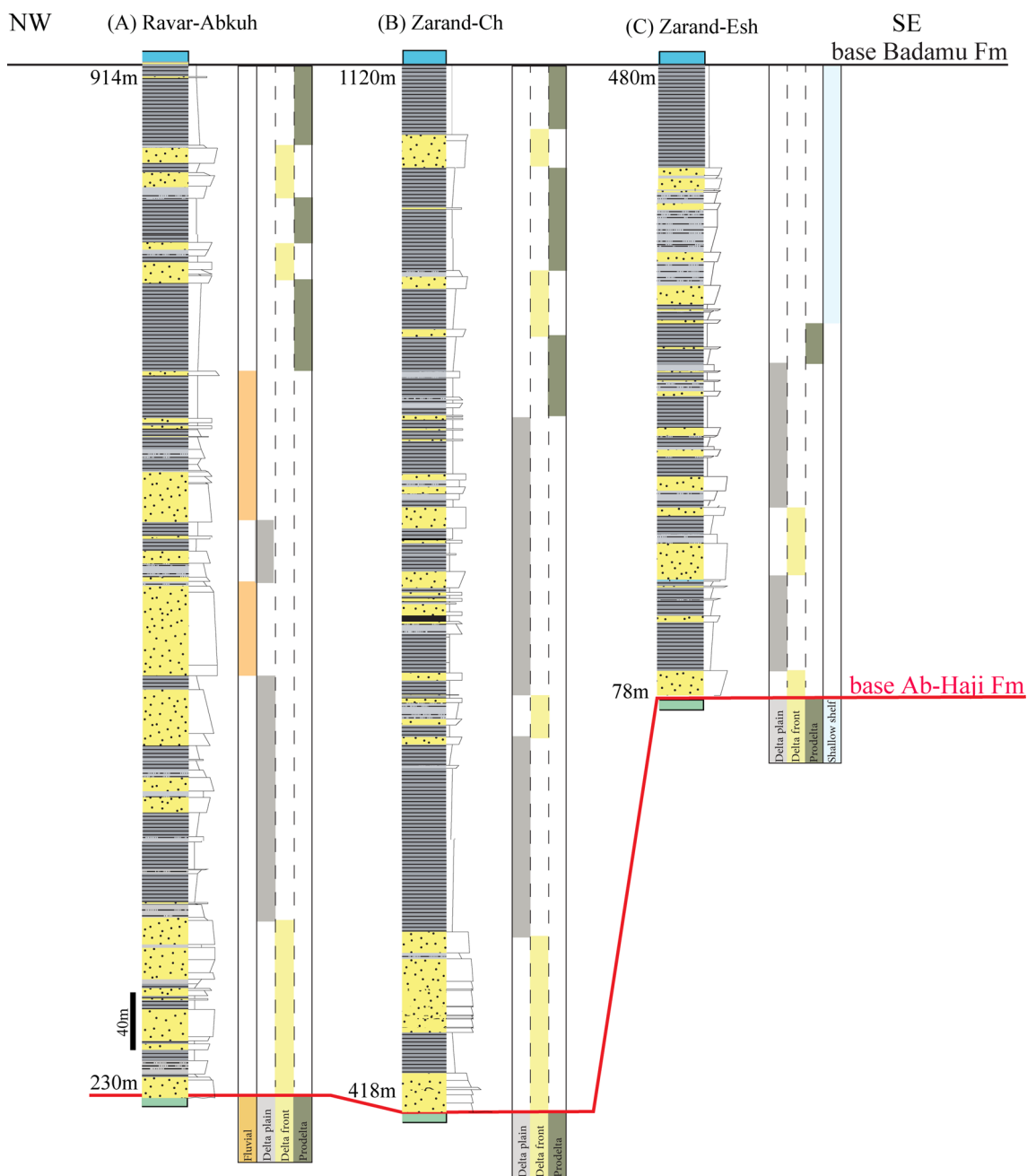
**Fig. 10** Vertical distribution of the five facies associations in the three stratigraphic sections studied herein

### 7.1 Correlation with other parts of the Iran Plate

The chronostratigraphy of the Ab-Haji Formation of the Tabas and Lut blocks is comparable to the Alasht Formation of the Shemshak Group in the Alborz Mountains of northern Iran (Fürsich et al. 2009a; Fig. 11). This interpretation results from the biostratigraphic studies carried out on the underlying Norian–Rhaetian Nayband Formation (Fürsich et al. 2005a) and the overlying Toarcian–Aalenian Badamu Formation (Seyed-Emami 1971; Seyed-Emami et al. 1993, 2000, 2004b). In the Alborz, lowermost

Jurassic molasse-type sediments (Alasht Formation in the south, lower Javaherdeh Formation in the north) overlie flysch-type Upper Triassic strata (characterizing the underfilled foreland basin) and seal Cimmerian foreland structures (Wilmsen et al. 2009b; Zanchi et al. 2009a). In the Binalud Mountains (NE Iran), the very-coarse-grained, non-marine Lower Jurassic siliciclastic strata of the Arefi and Bazehowz formations show large-scale fining-upward trends that reflect erosion of a high-relief source area down to the metamorphic basement that was deformed during the Late Triassic Eo-Cimmerian orogeny (Wilmsen et al.

**Fig. 11** Main lithostratigraphic units of the Upper Triassic–Jurassic succession of east-central Iran compared to the Alborz and Binalud mountains of northern and northeastern Iran. A, Main-Cimmerian unconformity; B, Mid-Cimmerian unconformity
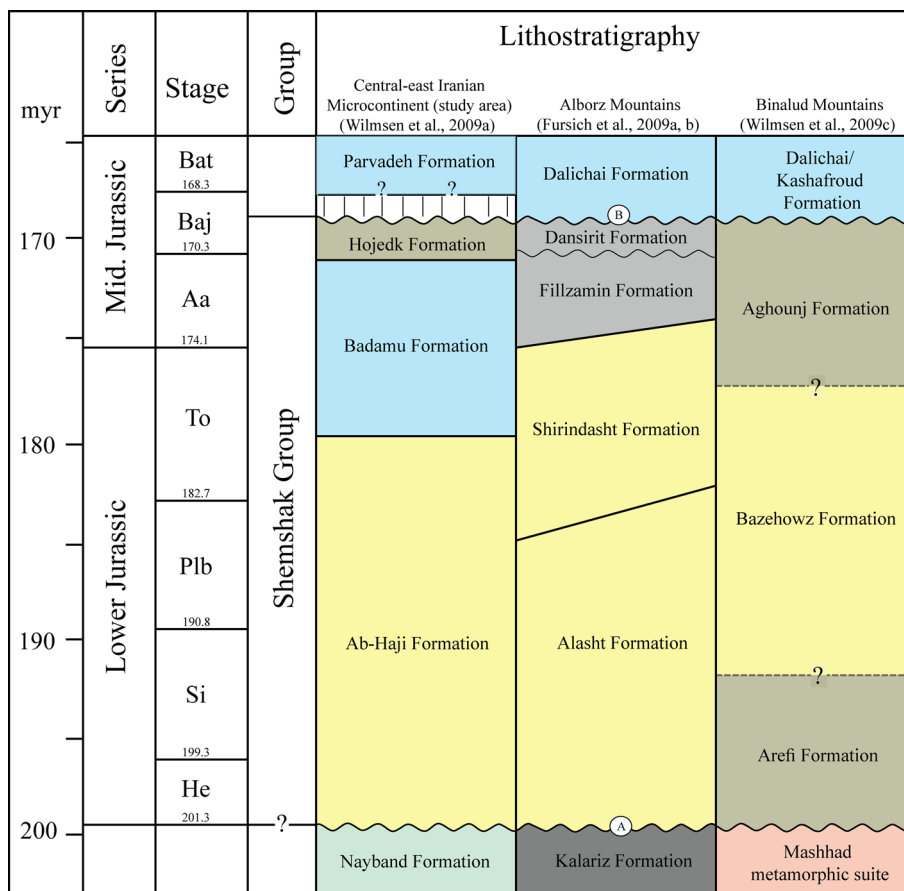


2009c; Zanchetta et al. 2013) (Fig. 11). Both the Lower Jurassic Shemshak Group in the Alborz and Binalud Mountains reflect the rapid uplift and denudation of the Cimmerian mountain chain with a north–south and northeast–southwest-directed transport of their erosional products. In the southern Tabas Block, fine-grained marine siliciclastics and limestones of the Upper Triassic Nayband Formation are abruptly replaced by coarse-grained siliciclastics at the Triassic–Jurassic boundary (Huckriede et al. 1962; Fürsich et al. 2005a). This general lithofacies pattern, i.e., a conspicuous and abrupt increase in the mean grain size of siliciclastic sediments in Central Iran (Tabas Block) is comparable to the situation in the Alborz and Binalud sequences at the Triassic–Jurassic boundary, indicating the generation of significant topography in the aftermath of the Eo- and Main-Cimmerian events (Wilmsen et al. 2009a, b, c). This event may have been triggered by slab break-off of the subducted Iran plate that has been inferred to have occurred at the Triassic–Jurassic boundary (Fürsich et al. 2009a; Wilmsen et al. 2009b) (Fig. 2b). Slab break-off usually follows continental collision and one of its consequence is rapid exhumation and erosion (e.g., Davies

and von Blanckenburg 1995). The tectono-stratigraphic evidence including flysch to molasses transition in peripherial foreland basin has been considered as a consequence of slab break-off (e.g. Sinclair 1997). The transition from an underfilled (flysch, lower Shemshak Group) to an overfilled (molasses, middle Shemshak Group) Alborz peripheral foreland basin was consequently explained by slab break-off following initial Cimmerian collision (Wilmsen et al. 2009b). The Cimmerian orogeny evidently had a big impact also on Central Iran as shown for example in the Anarak-Nakhlak and Posht-e-Badam areas (Bagherei and Stampfli 2008; Zanchi et al. 2009b). Thus, slab break-off may well have caused also rapid uplift and erosion in east-central Iran because of the coupling of the two plates. However, other geological evidence for this assumption such as syn- to post-collisional magmatism and metamorphism is still deserving additional investigation albeit Buchs et al. (2013) report poorly dated Late Triassic (?) retrograde metamorphism from blue- to greenshist conditions from the Anarak Metamorphic Complex, suggesting exhumation of the domain, most likely after slab detachment.
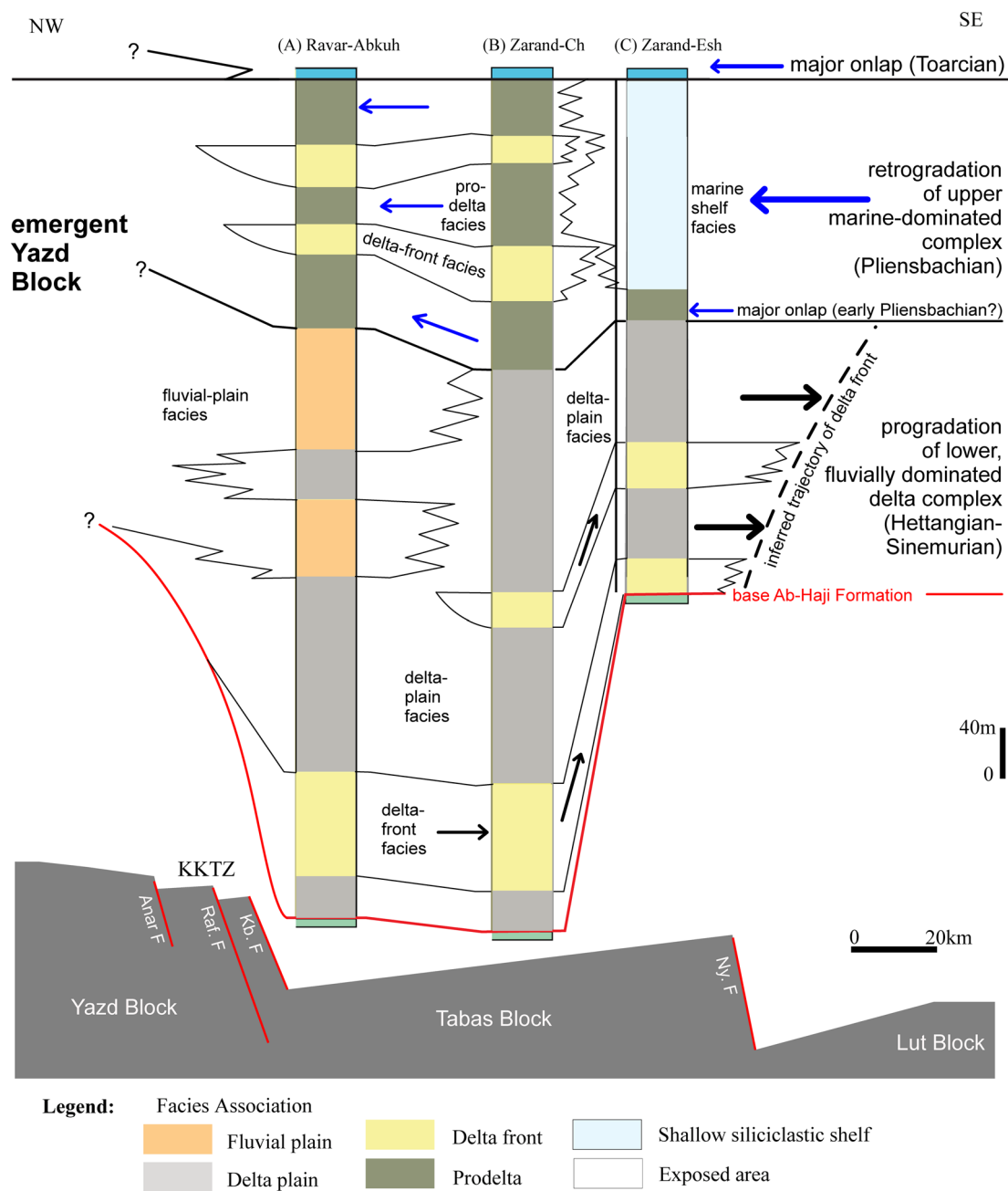
**Fig. 12** SE–NW transect of the reconstructed environments of the Lower Jurassic Ab-Haji Formation in the southern Tabas Block. From the SE, deltaic and shallow-marine environments (Zarand–Eshkeli section) grade into deltaic and fluvial settings towards the NW. Note the thickness variations and facies changes from SE to NW that follow the pattern of basement uplift and erosion of tilted fault blocks. *KKTZ* Kashmar–Kerman Tectonic Zone, *Kb* Kuh Banan, *Raf* Rafsanjan, *Ny* Nayband

## 7.2 Facies development and thickness changes

In the southern Tabas Block (Ravar-Zarand area), the Ab-Haji Formation reaches up to 702 m in thickness. At Ravar–Abkuh, the basal 120 m of the Ab-Haji Formation (684 m in total) are represented by coarsening-upward delta-plain to delta-front sandstones, overlain by 360 m of fluvial and delta-plain sediments which grade up-section into 204 m of delta-front and prodelta deposits (Fig. 12). At Zarand–Chenaruyeh, the Ab-Haji Formation has nearly the same thickness (702 m) as in the Ravar area (Fig. 12). The base of the formation shows a similar, coarsening-upward delta plain to delta-front facies succession. The delta-front facies is capped by 110 m of fine-grained delta plain deposits. These are followed by several, in total 170-m-thick coarsening-upward delta-front sequences

within finer-grained delta plain deposits. The remaining part of the Sect. (275 m) mainly consists of prodelta deposits with two coarsening-upward delta-front sandstone packages. This section shows a similar shallowing- and deepening-trend as the Ravar–Abkuh section, but the fluvial-plain deposits in the middle part of the formation at the latter section are replaced by delta-front sediments. Ten kilometers towards the SE, at Zarand–Eshkeli, the Ab-Haji Formation thins to 402 m. It starts with 15 m of coarsening-upward delta-front sandstones (Fig. 12), followed by 60 m of fine-grained delta plain deposits which grade upwards into a 100 m-thick package consisting of three coarsening-upward delta-front sandstones within finer-grained delta plain deposits. The remaining succession is composed of 165 m of prodelta shale and shallow-marine sandstone. The Ab-Haji Formation ends with a 65-m-thick succession of laminated marine shale. In this section, the fluvial plain or thick delta-front deposits are absent and are replaced by deeper-water prodelta and shallow-siliciclastic-shelf strata (Fig. 12). The Ab-Haji Formation of the Kerman area, 85 km towards the SE, is only 25 m thick and composed of a fully marine siliciclastic sediment package (Fürsich et al. 2005a). The strong progradation of the delta-front sandstones at sections (A) and (B) (Ravar–Abkuh and Zarand–Chenaruyeh) towards the east-southeast indicates the predominance of fluvial processes. Thus, the Ab-Haji delta system in the southern Tabas Block appears to be fluvial-dominated (Figs. 12, 17). It is worth noting that the general facies evolution of the Ab-Haji Formation during the Early Jurassic closely corresponds to the trends seen in the contemporaneous Alasht Formation of the southern Alborz Mountains (Fürsich et al. 2009a). The latter formation overlies shallow-marine to paralic strata of the Norian–Rhaetian Shamirzad and Kalariz formations with a sharp increase in grain size and is dominated in its lower (Hettangian–Sinemurian) part by fluvial strata. In the upper (Pliensbachian–Lower Toarcian) part, the Alasht Formation becomes finer grained. Coastal-plain environments prevail and marine ingressions are indicated by trace fossils horizons and shell beds with marine fossils. A major deepening event in the Toarcian–Aalenian, corresponding to the deposition of the shelf and slope deposits of the Shirindasht and Fillzamin formations in the Alborz Mountains (Fürsich et al. 2005b, 2009a), is reflected by the condensed, ammonite-rich limestones and marls of the Badamu Formation on the Tabas and Lut blocks (Seyed-Emami 1971; Wilmsen et al. 2009a). This general synchronicity in facies development suggest a common tectono-stratigraphic framework for the deposition in both areas, and, albeit detailed biostratigraphic data for the Ab-Haji Formation are lacking, it may be speculated that the

prograditional lower, fluvio-deltaic complex of the formation may be Hettangian–Sinemurian in age while the retrogradational upper part may correspond to the Pliensbachian.

The Ab-Haji Formation thickens toward the southern Tabas Block and reaches its maximum thickness in the Ravar-Zarand area ("Zarand Trough" of Huckriede et al. 1962) (Fig. 6a–c). However, the thickness of the formation decreases very rapidly from 700 m in the Ravar-Zarand area to only several tens of meters towards the southeast in the Kerman area (Fürsich et al. 2005a). The sedimentary environments also change from fluvial and deltaic in the west (Ravar area) to shallow marine in the southeast (Zarand–Eshkeli and Kerman region). Palaeocurrent analyses in the two southern sections (Ravar–Abkuh and Zarand–Chenaruyeh) also show unimodal patterns with a mean flow direction to the east and southeast (Fig. 17). The great thickness of the formation in the Ravar-Zarand area points to high subsidence of the southern Tabas Block, adjacent to a high-relief and emergent southern Yazd Block (Fig. 12).

In order to show the subsidence and uplift history of the southern Tabas Block sedimentary basin since the Early Jurassic, subsidence curve were generated based on stratigraphic data collected from the three outcrops in this area (Fig. 13). Due to the lack of well calibrated biostratigraphic data, the general thicknesses of the Hettang–Sinemurian and the Pliensbachian of the Ab-Haji Formation as well as the Toarcian–Aalenian of the Badamu Formation were plotted for the three sections. Based on the subsidence curves plotted for the tectonic domain of the southern Tabas Block, this part of basin subsided along block faults from the Early Jurassic. The subsidence curves show a relatively high and rapid subsidence rate in the Early Jurassic that confirms the onset of extension in this time (Fig. 13). In addition, the subsidence rates in western part of southern Tabas Block (Ravar–Abkuh, Zarand–Chenaruyeh), was decreasing towards the east (Zarand–Eshkeli). During Toarcian–Aalenian times, tectonic subsidence rate was lower as the curves flatten in this interval, and finally in the Early Bajocian (Hodjek Formation), subsidence rates dramatically increases again in the run-up to the Mid-Cimmerian Event (Fig. 13).

The observed pattern of facies and thickness changes in this area are evidence of strong differential subsidence with a proximity of erosional areas and depocenters which may best be explained by an array of tilted fault blocks (e.g., Leeder and Gawthorpe 1987). Salehi et al. (2014a) indicated that a series of extensional, fault-bounded tilted blocks readily explained the observed thickness variations and rapid east-to-west facies changes of the Ab-Haji Formation on the Yazd, northern Tabas and Lut blocks (see Fig. 1 for location).

**Fig. 13** Early to early Middle Jurassic subsidence curves for the three studied sections
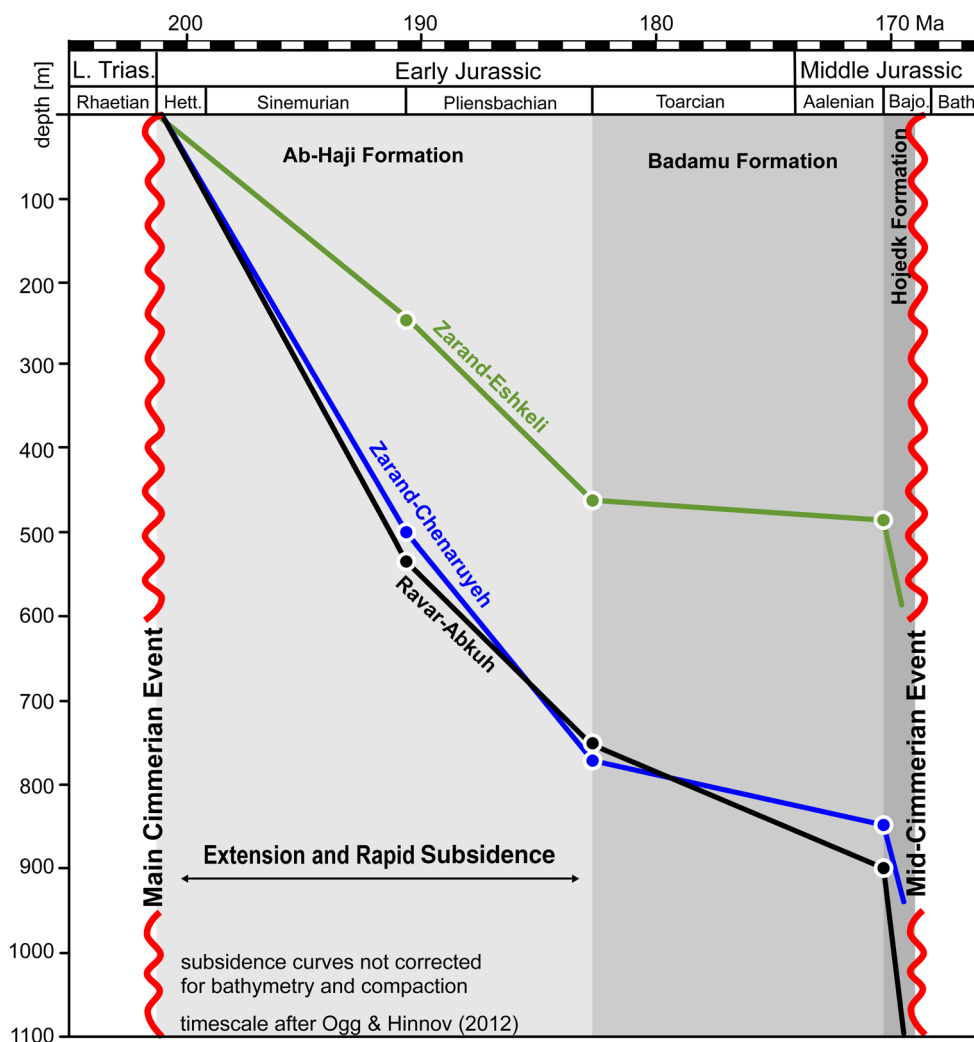


## 7.3 Source areas

The source areas of the siliciclastic sediments of the Ab-Haji Formation can be reconstructed based on thickness variations, lateral facies changes, changes in the type of the basal contact, and by petrographic provenance studies. Salehi et al. (2014b) reported detailed lithological descriptions, modal analyses on forty-two sandstone samples collected along the measured stratigraphic sections and whole-rock geochemistry were performed on 32 sandstone and 16 shale samples to obtain analytical data for major, trace and rare earth elements of the Ab-Haji Formation; here, only the main results of this study are briefly summarized in order to compose a comprehensive picture of palaeogeographic and geodynamic framework of the formation.

Sandstone modal analysis shows that the sandstones of this formation on the western and southern Tabas Block (Kuh-e-Rahdar, Ravar–Abkuh and Zarand–Chenaruyeh sections) consist of submature litharenites (phyllarenites

and sedarenites) to sublitharenites with predominant sedimentary and low-grade metamorphic grains while the sandstones of the eastern Tabas and western Lut blocks (Parvadeh and Kuh-e-Shisui sections) consist of mineralogically mature quartz-rich sublitharenites (Fig. 14a–d; Table 3). Such compositions document provenance from recycled-orogen field (Fig. 15).

Sedimentary and (meta-)sedimentary grains occur in variable proportions throughout the Ab-Haji sandstones in the western Tabas Block while volcanic lithics (Lv) are absent. Geochemical data indicate that the Ab-Haji sediments were derived from a mixed sedimentary or (meta-)sedimentary source. (Meta-)sedimentary lithics (low-grade metamorphic), including slate and phyllite, are dominating grain types in the western Tabas Block (Shadan and Hosseini-Barzi 2013; Salehi et al. 2014b) (Fig. 14a, b). Variations in sedimentary rock fragments as well as low-grade metamorphic rock fragments of the Kuh-e-Rahdar, Ravar–Abkuh and Zarand–Chenaruyeh sections point to derivation of grains from a recycled-orogen provenance
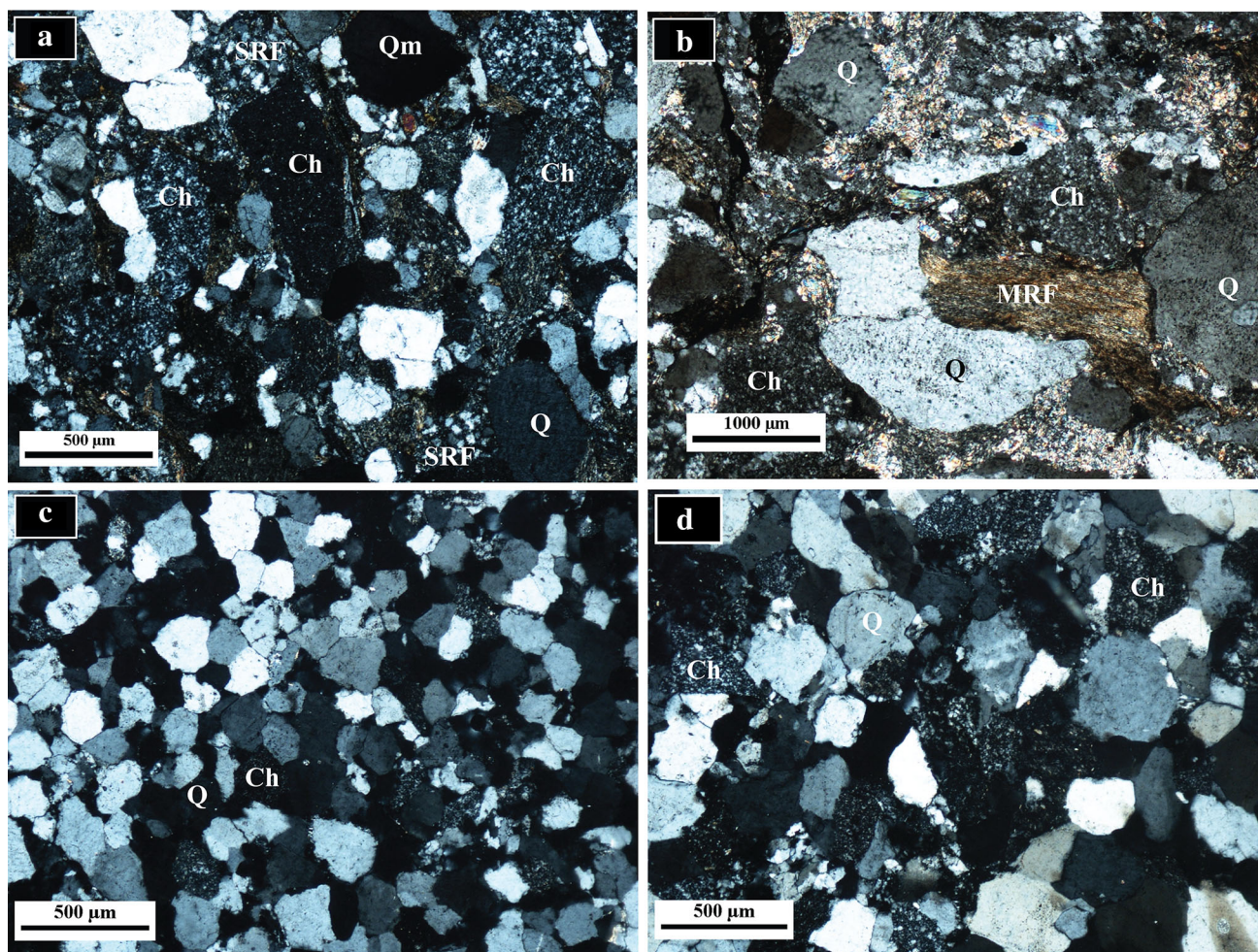
**Fig. 14** Representative photomicrographs of selected sandstone samples of the Ab-Haji Formation. **a** siltstone rock fragment (SRF), monocrystalline quartz (Q), and chert (Ch) in submature litharenite. Ravar–Abkuh Sample. **b** Metamorphic rock fragments (MRF), monocrystalline quartz (Q), and chert (Ch) in submature phyllitharenite. Kuh-e-Rahdar Sample. **c** Monocrystalline quartz (Q), and chert (Ch) in mature quartz-rich sublitharenite. **d** Chert grains (Ch) in mature chertarenite. C and D Parvadeh Sample. All photos with crossed polars

**Table 3** Mean of major grains (Qt, F and L) and frequent petrofacies of selected sandstone samples from the Ab-Haji Formation in east central Iran

|  | Outcrop name | Outcrop no. | N. S. | Qm | Lt | F | Petrofacies; Folk (1980) |
|---|---|---|---|---|---|---|---|
| 1 | Ravar–Abkuh | A | 9 | 53 | 44 | 3 | Phyillarenite |
| 2 | Zarand–Chenaruyeh | B | 6 | 54 | 41 | 4 | Sedarenite to phyillarenite |
| 3 | Kuh-e-Rahdar | D | 6 | 38 | 61 | 1 | Phyllarenite |
| 4 | Simin-Sepahan | E | 8 | 31 | 66 | 3 | Sedarenite |
| 5 | Parvadeh | F | 7 | 68 | 30 | 2 | Sublitharenite to chertarenite |
| 6 | Kuh-e-Shisui | G | 6 | 81 | 15 | 4 | Sublitharenite |

from the west-dipping tilted Yazd Block (including the long, arcuate and structurally complex belt in eastern Yazd Block defined as KKTZ; Haghipour and Pelissier 1977) and their transport to the western and southern Tabas Block (Fig. 12).

Modal analysis of sandstones and geochemistry of sandstones and shales suggest a derivation from pre-Jurassic plutonic, metamorphic and quartzose sedimentary source rocks within a recycled-orogen tectonic setting for the western and southern Tabas Block. Within recycled orogens, sediment sources are predominantly sedimentary

Fig. 15 QmFLt plots for tectonic provenance of sandstones from the Ab-Haji Formation (modified after Salehi et al. 2014b). The grey arrow highlights the compositional trend from litharenite to sublitharenites recorded during the unroofing and recycling of the exposed rocks of the tilted Yazd and Tabas blocks. Provenance fields after Dickinson and Suczek (1979). Black circles mark samples from sections A–B and D–E, white circles from sections F–G (see Fig. 1b for location)
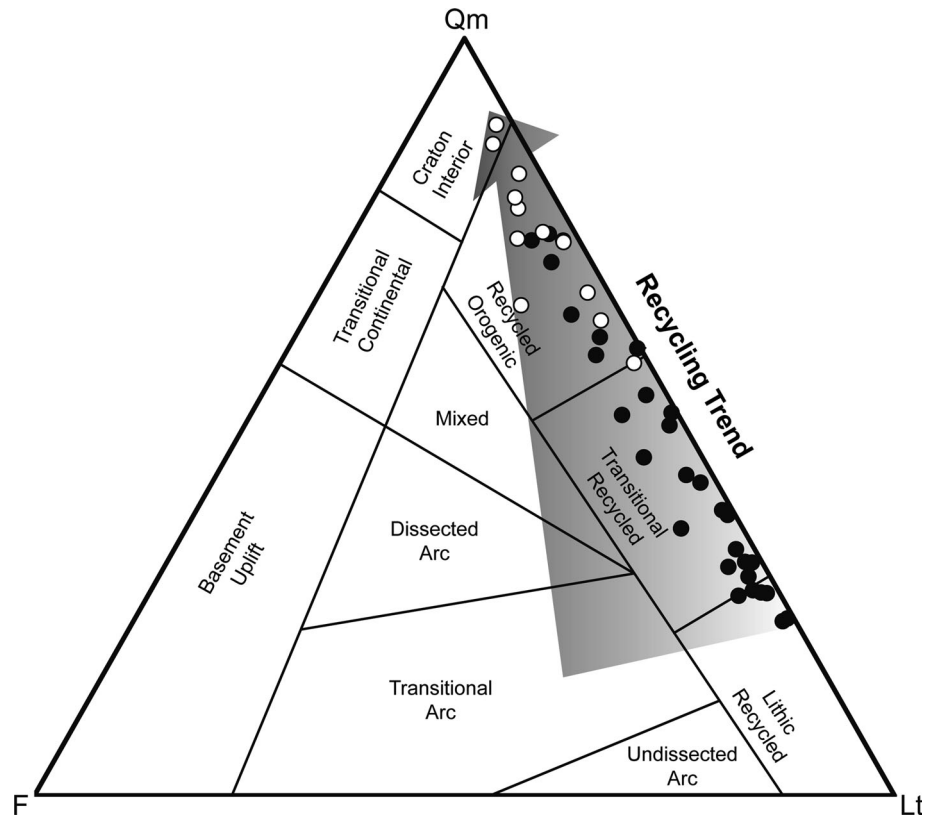
rocks and derived from tectonic settings in which stratified rocks were deformed, uplifted and eroded. The exposed zones in western east-central Iran yielded sediments of recycled-orogen character where strata had been consolidated by the Eo-Cimmerian orogeny (Masoodi et al. 2013).

The composition of sandstones from the Ab-Haji Formation suggests sources that likely include Precambrian and Ordovician–Triassic sedimentary, low-, middle- and upper-rank metamorphic and plutonic rocks of the Yazd Block, i.e., the KKTZ. Several metamorphic complexes in the western and northwestern part of the Yazd Block are attributed to the Variscan to Eo-Cimmerian tectonic evolution of the Palaeotethys margin (Aghanabati 2004; Bagheri and Stampfli 2008; Zanchi et al. 2009b; Masoodi et al. 2013). Block movements resulted in uplift and erosion of the exposed rocks, including metamorphic complexes of the Precambrian, Ordovician to Triassic rocks of the eastern Yazd Block (i.e., the KKTZ) (Aghanabati 2004). Local erosion down to Lower Palaeozoic levels on the Yazd Block confirms a phase of uplift and erosion (Eo-Cimmerian orogeny; Bagheri and Stampfli 2008). The Upper Neoproterozoic and Lower Palaeozoic rocks, including plutonic-metamorphic rocks of the Bayazeh and Sagand areas (Boneh Shurow complex: Bagheri and Stampfli 2008; Kargaranbafghi et al. 2015) as well as the Posht-e-Badam complex (Kargaranbafghi et al. 2012, 2015) of the KKTZ in the eastern Yazd Block which

had become exposed during the Eo-Cimmerian orogenic phase are potential source rocks for the Ab-Haji Formation of the western Tabas Block (Salehi et al. 2014b) (Fig. 16).

Masoodi et al. (2013) considered the Neotethys arc as a continental arc and/or collisional granitic intrusions during the Eo-Cimmerian Orogeny with its position between the Yazd and Tabas blocks (KKTZ). However, the expected magmatic-arc-related provenance is not detected in modal or geochemical analyses of the Ab-Haji Formation on the Tabas Block (Shadan and Hosseini-Barzi 2013; Salehi et al. 2014b). The source area of siliciclastic material of the northeastern Tabas and the Lut blocks could have been the subaerially exposed eastern part of the Tabas Block, i.e., an area approximately parallel to the present-day strike of the Shotori Mountains (the so-called Shotori Horst/Swell; Stöcklin and Nabavi 1971) (Figs. 16, 17). A similar source area was considered for the Callovian (Middle Jurassic) syntectonic siliciclastic rocks of the Sikhor Formation, which were deposited along the Nayband Fault at the eastern margin of the Tabas Block (Fürsich et al. 2003). A proximal source area has also been assumed for thick siliciclastic strata in the underlying Nayband Formation on the eastern margin of the Tabas Block (Fürsich et al. 2005a).

There is evidence for synsedimentary uplift and erosion at several localities in the southern Shotori Mountains (Fig. 1b). For example, east of Kuh-e-Jamal, the Upper
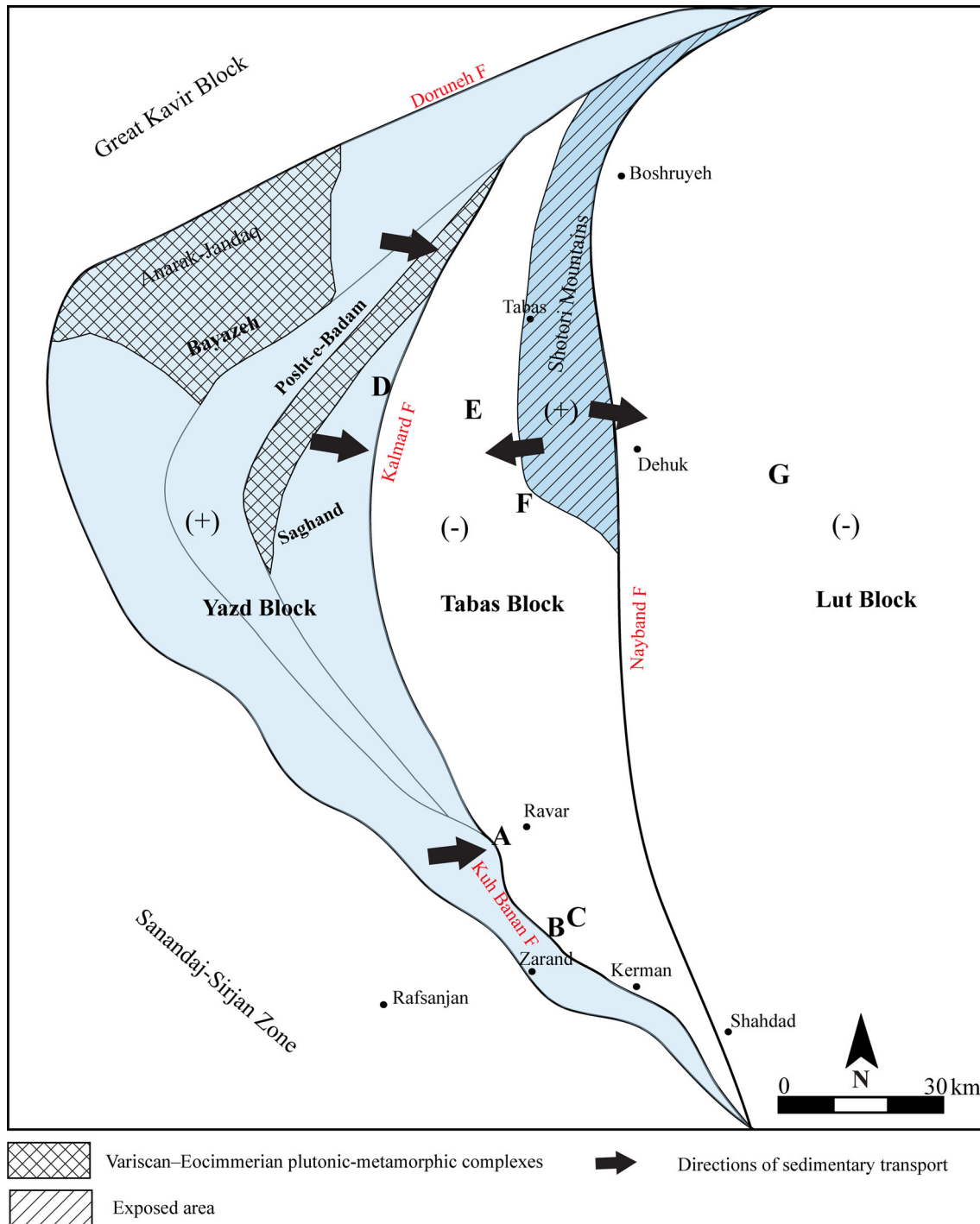
**Fig. 16** Potential source area and sediment transport directions for the Ab-Haji Formation in east-central Iran during the Early Jurassic. Blue areas marked by (+) display the assumed uplifted source area while areas marked by (−) indicate zones of subsidence (modified after Salehi et al. 2014b). Blocks and block-bounding faults modified from Wilmsen et al. (2009b)

Bajocian–Bathonian Parvadeh Formation unconformably overlies Permian quartzites. This points to a major hiatus and to one or several phases of uplift and erosion of the Shotori Swell (Stöcklin and Nabavi 1971; Fürsich et al. 2009b; Wilmsen et al. 2009a). Stöcklin and Nabavi (1971) interpreted the Shotory range, for the first time, as a horst

forming a swell during the Late Triassic and Jurassic. In yet other areas in the southern Shotori Mountains (e.g., north of the road from Tabas to Esfak and southwest of Esfak), the Ab-Haji Formation is missing entirely so that the Badamu Formation directly overlies the Permian Khan and Esfak limestones (Fürsich, unpubl. data). Based on the
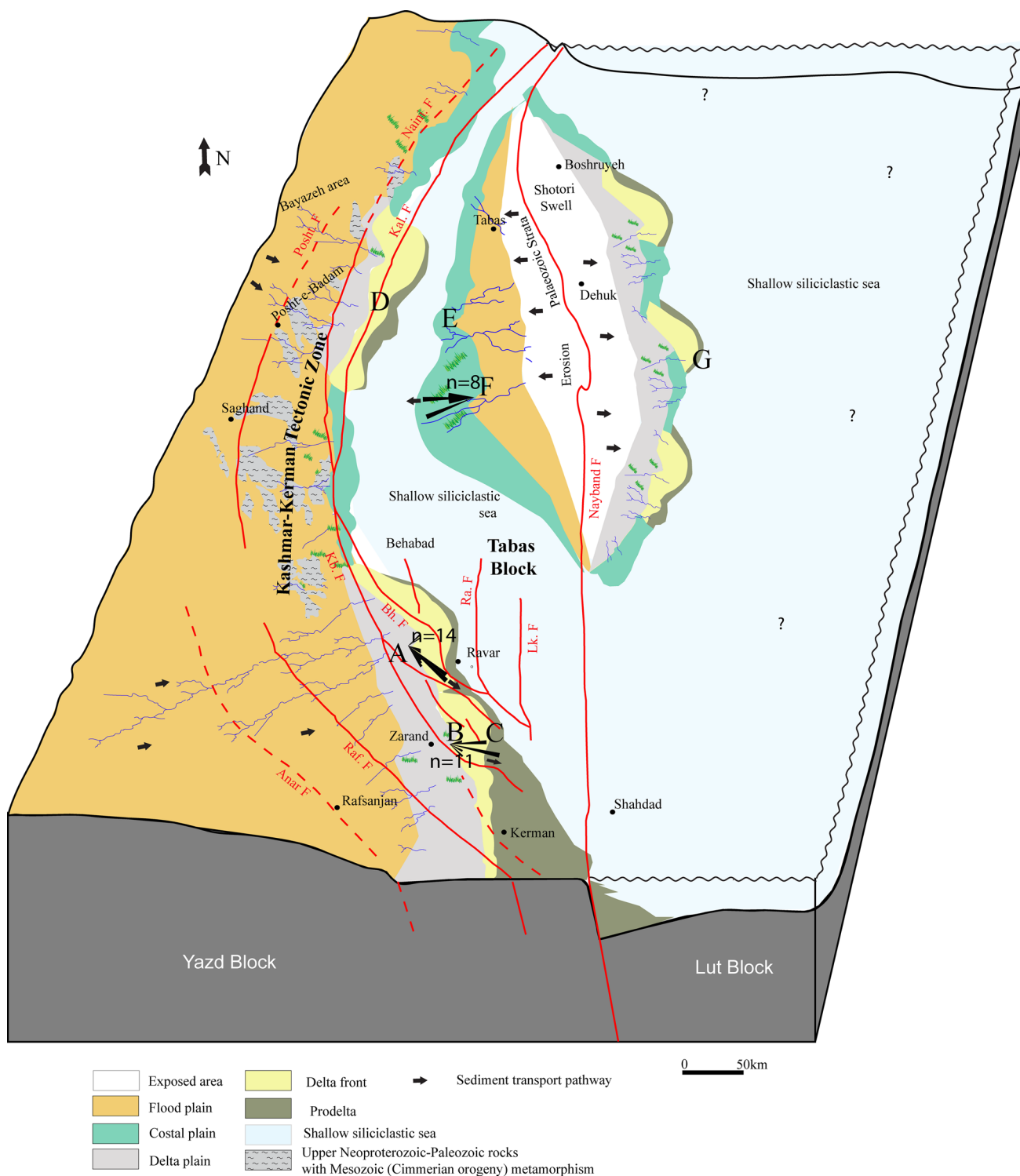
**Fig. 17** Palaeogeography of east-central Iran (blocks and faults; modified from Zamani-Pedram (2011). A–C refer to Ravar–Abkuh (A), Zarand–Chenaruyeh (B), and Zarand–Eshkeli (C) and D–G refer to previously measured sections (Salehi et al. 2014a) of the Kuh-e-Rahdar (D), Simin-Sepahan (E), Parvadeh (F) and Kuh-e-Shisui (G) areas, respectively. Major strike-slip or reverse faults of central and eastern Iran: *Kal* Kalmard, *Posht* Posht-e-Badam, *Raf* Rafsanjan, *Kb* Kuh Banan, *Bh* Behabad, *Ra* Ravar, *Lk* Lakar Kuh. Rose diagrams represent palaeocurrents, *n* indicates the number of palaeocurrent measurements at each site. Circles indicate major cities

evidence of synsedimentary removal of strata, the silici-clastic strata of the Ab-Haji Formation in the northeastern Tabas and western Lut Block are mainly derived from Late Palaeozoic and Triassic sedimentary strata of the Shotori Swell. The compositional trend with the progressive increase of quartz within the Ab-Haji sandstones of Parvadeh and Kuh-e-Shisui highlights the erosion and recycling of older quartz-rich sedimentary rocks of tilted Tabas blocks in comparison with more lithic-rich of the sandstones from the outcrops adjacent to the Yazd Block (Fig. 15).

Palaeogeographic reconstructions by Barrier and Vrielynck (2008) indicate volcanic activity at the active margin of the Lut Block during the Norian. This volcanic activity is interpreted as the result of subduction of the Neotethys oceanic crust beneath Central Iran which led to the formation of an extensional continental back-arc basin in east-central Iran in the late Triassic (Wilmsen et al. 2009b). The shallow angle of Neotethys subduction beneath SW Iran (Ghasemi and Talbot 2006) caused both the limited volcanic activity in the arc (on the Lut Block) and the very broad extensional back-arc zone. This activity resulted in the development of major syndepositional normal faults in east-central Iran (Fig. 2a). This type of basin commonly shows a steep, thrust-faulted arc-ward margin and a more gentle-dipping, block-faulted inner craton–ward margin (Einsele 2000). The lack of volcanic lithic grains in the Ab-Haji Formation can thus be explained by the low volcanic activity of this arc during the Early Jurassic, by the significant distance between the inferred volcanic arc at the eastern margin of the Lut Block and the Ab-Haji basin, by a high degree of sedimentary recycling, by intensive chemical weathering in the source area (Salehi et al. 2014b), or a combination of the above.

## 7.4 Geodynamic significance and palaeogeography

The Eo-Cimmerian orogeny transformed northern Iran into a compressional or transpressional tectonic setting (Wilmsen et al. 2009b) and Zanchi et al. (2016) presented geological evidence for oblique convergence during the Cimmerian collision. Shortly after the collision and closure of the Palaeotethys in early Late Triassic times (late Carnian/early Norian; Horton et al. 2008), Neotethys subduction started at the southern margin of Iran still within the Late Triassic (Arvin et al. 2007). This process reduced compressional stress in this region so that extensional post-collisional basins could form (cf. Brunet et al. 2003; Fürsich et al. 2005a). The following geological, stratigraphic, and sedimentological data from the Ab-Haji Formation support an extensional setting in east-central Iran:

- Extensional tectonic pulses were documented by numerous sedimentologic and stratigraphic data in east-central Iran during the Late Triassic to Late Jurassic (Fürsich et al. 2003, 2005a; Seyed-Emami et al. 2004a; Wilmsen et al. 2010; Cifelli et al. 2013). Shahidi et al. (2007, 2010) also associated the deposition of the thick sequence of the "Shemshak Formation" (i.e. the Shemshak Group) in northern and central Iran to the activity of major syndepositional normal faults (see also Toarcian reconstruction of the area by Barrier and Vrielynck 2008; Fig. 2a). Furthermore, also Fürsich et al. (2005b) reported a major Toarcian–Aalenian rifting event in the Alborz Mountains.

- Strongly deformed pre-Jurassic rocks, thrust stacks with sharp unconformities, and/or angular unconformities indicate a compressional or transpressional tectonic setting in northern and northeastern Iran (Zanchi et al. 2009a, 2016) but this evidence has not been documented below the Nayband or Ab-Haji formations in east-central Iran (Fürsich et al. 2005a; Wilmsen et al. 2009a).

- The thickness of the Ab-Haji Formation varies considerably throughout the basin both along strike and in a direction perpendicular to the major block boundaries. Its thickness is highest in the axis of maximum tectonic subsidence, decreases to a few tens of meters laterally and is reduced to nil toward its uplifted margin.

- The Ab-Haji Formation displays significant lateral facies changes. Fine-grained lithofacies prevail in the areas of maximum tectonic subsidence of the basin and give way to coarser fluvial facies toward the uplifted margins. Additional facies evidence is provided by the deltaic lobes that migrate towards the axis of maximum tectonic subsidence.

- Arc-related provenance signatures have not been detected in the Ab-Haji sandstone, while a continental back-arc setting which shows a steep, thrust-faulted arc-ward margin and a more gently dipping, block-faulted inner craton-ward margin is more probable. The dominant recycled-orogen provenance for the Ab-Haji sandstones is inherited from exposures of supracrustal successions that formed during the Eo-Cimmerian orogenic phase at the end of the Triassic and provided the principal sediment supply from the west (i.e., KKTZ) to the Ab-Haji Basin during the Early Jurassic.

The basinwide changes observed in thickness and facies as well as the provenance and presence of onlapping geometries without extensive sharp unconformities can be best explained by normal faulting. They are a plausible consequence of sedimentation across tilted fault blocks in an extensional basin (e.g., Leeder and Gawthorpe 1987).

# 8 Conclusions

1. The Lower Jurassic Ab-Haji Formation was deposited across tilted fault blocks of the CEIM. It reaches a thickness of up to 700 m in the southern Tabas Block where it shows the most complete and well exposed sections. It is locally reduced to a few tens of meters towards the southeast and disappears on the Shotori Swell at the eastern margin of the Tabas Block.

2. Lithofacies analysis of three well-exposed outcrop sections resulted in the recognition of thirteen lithofacies and five facies associations that are interpreted as representing (1) fluvial (2) delta plain, (3) delta front, (4) prodelta, and (5) shallow-marine shelf environments. The Ab-Haji delta system in the southern Tabas Block appears to be fluvially dominated.

3. The Ab-Haji Formation shows a distinct increase in grain size of the siliciclastic sediments near the Triassic–Jurassic boundary, similar to the successions in the Alborz and Binalud mountains of northern and northeastern Iran. This tectonostratigraphic signal may have been triggered by the Main-Cimmerian event in northern Iran (slab break-off?), causing tectonic instability associated with uplift and erosion also in the study area.

4. The observed pattern of rapid SE–NW directed facies and thickness changes across the southern Tabas Block of the CEIM is evidence of strong differential subsidence in response to block-tilting with a close association of erosional areas and depocenters. Based on geohistory analysis, after the main Cimmerian event, the southern Tabas Block basin subsided during the Early Jurassic which confirm extensional tectonic setting during the deposition of the Ab-Haji Formation.

5. Exposure of supracrustal successions, including plutonic-metamorphic and sedimentary rocks on the elevated western Yazd Block due to the Eo-Cimmerian orogenic phase at the end of the Triassic, provided a westerly source area for the western Tabas Block. In contrast, the most plausible source areas for the eastern Tabas Block and western Lut Block are the exposed sedimentary strata on the Shotori Swell (the uplifted crest of the eastern Tabas Block).

6. The basinwide changes observed in thickness and the rapid east–west facies changes as well as the provenance can best be explained by normal faulting across tilted fault blocks in an extensional basin during the Early Jurassic. Extension resulted in west-dipping fault blocks, differing regionally in degree of subsidence and synsedimentary movements and producing large half-grabens. This general geodynamic setting is strongly supported by the geological, stratigraphic, and sedimentological evidence from the integrated study of the Ab-Haji Formation across a large area of east-central Iran.

# References

Aghanabati, S. A. (2004). Geology of Iran. *Geological Survey of Iran*, pp. 587 (**in Persian**).

Alavi, M., Vaziri, H., Seyed-Emami, K., & Lasemi, Y. (1997). The Triassic and associated rocks of the Nakhlak and Aghdarband areas in central and northeastern Iran as remnants of the southern Turanian active continental margin. *Geological Society of America Bulletin, 109,* 1563–1575.

Arvin, M., Pan, Y., Dargahi, S., Malekizadeh, A., & Babaei, A. (2007). Petrochemistry of the Siah-Kuh granitoid stock southwest of Kerman, Iran: implications for initiation of Neotethys subduction. *Journal of Asian Earth Sciences, 30,* 474–489.

Bagheri, S., & Stampfli, G. M. (2008). The Anarak, Jandaq and Poshte-Badam metamorphic complexes in central Iran: New geological data, relationships and tectonic implications. *Tectonophysics, 451,* 123–155.

Barrier, E., & Vrielynck, B. (Eds.) (2008). Palaeotectonic maps of the Middle East—tectono-sedimentary–palinsspastic maps from the Late Norian to Pliocene. Commission for the Geological Map of the World (CGMW/CCGM), Paris.

Besse, J., Torcq, F., Gallet, Y., Ricou, L. E., Krystyn, L., & Saidi, A. (1998). Late Permian to Late Triassic palaeomagnetic data from Iran: constraints on the migration of the Iranian block through the Tethyan Ocean and initial destruction of Pangaea. *Geophysical Journal International, 135,* 77–92.

Bhattacharya, J. P. (2006). Deltas. In H. W. Posamentier, & R. G. Walker (Eds.), Facies models revisited (pp. 237–292). *Society for Sedimentary Geology (SEPM) Special Publication,* 84. Tulsa: Society for Sedimentary Geology.

Brunet, M.-F., Korotaev, M. V., Ershov, A. V., & Nikishin, A. M. (2003). The South Caspian Basin: a review of its evolution from subsidence modelling. *Sedimentary Geology, 156,* 119–148.

Buchs, D. M., Bagheri, S., Martin, L., Hermann, J., & Arculus, R. (2013). Paleozoic to Triassic ocean opening and closure preserved in Central Iran: Constraints from the geochemistry of meta-igneous rocks of the Anarak area. *Lithos, 172–173,* 267–287.

Cant, D. J., & Walker, R. G. (1976). Development of a braided-fluvial facies model for the Devonian Battery Point Sandstone, Quebec. *Canadian Journal of Earth Sciences, 13,* 102–119.

Cifelli, F., Mattei, M., Rashid, H., & Ghalamghash, J. (2013). Right-lateral transpressional tectonics along the boundary between Lut and Tabas blocks (Central Iran). *Geophysical Journal International, 193,* 1153–1165.

Coleman, J. M. (1988). Dynamics changes and processes in the Mississippi Delta. *Geological Society of America Bulletin, 100,* 999–1015.

Coleman, J. M., & Prior, D. B. (1982). Deltaic environments of deposition. In P. A. Scholle, & D. Spearing (Eds.), Sandstone depositional environments (pp. 139–178). *American Associationof Petroleum Geologists, Memoir,* 31. Tulsa: American Association of Petroleum Geologists.

Collinson, J. D. (1996). Alluvial sediments. In H. G. Reading (Ed.), *Sedimentary environments: process, facies and stratigraphy* (pp. 37–82). Oxford: Blackwell Scientific Publications.

Davies, J. H., & von Blanckenburg, F. (1995). Slab breakoff: A model of lithospheric detachment and its test in the magmatism and deformation of collisional orogens. *Earth and Planetary Science Letters, 129,* 85–102.

Davoudian, A. R., Genser, J., Neubauer, F., & Shabanian, N. (2016). 40Ar/39Ar mineral ages of eclogites from North Shahrekord in the Sanandaj-Sirjan Zone, Iran: Implications for the tectonic evolution of Zagros orogen. *Gondwana Research, 37,* 216–240.

Davoudzadeh, M., Soffel, H., & Schmidt, K. (1981). On the rotation of the Central-East Iran microplate. *Neues Jahrbuch für Geologie und Paläontologie - Monatshefte, 3,* 180–192.

Dickinson, W. R., & Suczek, D. R. (1979). Plate tectonics and sandstone compositions. *American Association of Petroleum Geologists Bulletin, 63,* 2164–2182.

Einsele, G. (2000). *Sedimentary basins: evolution, facies, and sediment budget* (p. 792). Berlin: Springer.

Elliott, T. (1986). Deltas. In H. G. Reading (Ed.), *Sedimentary environments and facies* (pp. 113–154). Oxford: Blackwell.

Esmaeily, D., Bouchez, J. L., & Siqueira, R. (2007). Magnetic fabrics and microstructures of the Jurassic Shah-Kuh granite pluton (Lut Block, Eastern Iran) and geodynamic inference. *Tectonophysics, 439,* 149–170.

Farrell, K. M. (1987). Sedimentology and facies architecture of overbank deposits of the Mississippi River, False River Region, Louisiana. In F. G. Ethridge, R. M. Flores, & M. D. Harvey (Eds.), *Recent developments in fluvial geology* (pp. 111–120). *Society for Sedimentary Geology (SEPM) Special Publications,* 39. Tulsa: Society for Sedimentary Geology.

Folk, R.L. (1980). Petrology of sedimentary rocks (p. 182). Austin: Hemphill Publishing Co.

Fürsich, F. T., Hautmann, M., Senowbari-Daryan, B., & Seyed-Emami, K. (2005a). The Upper Triassic Nayband and Darkuh formations of east-central Iran: stratigraphy, facies patterns and biota of extensional basins on an accreted terrane. *Beringeria, 35,* 53–133.

Fürsich, F. T., Wilmsen, M., Seyed-Emami, K., Cecca, F., & Majidifard, M. R. (2005b). The upper Shemshak Formation (Toarcian-Aalenian) of the Eastern Alborz (Iran): Biota and palaeoenvironments during a transgressive-regressive cycle. *Facies, 51*(1–4), 365–384.

Fürsich, F., Wilmsen, M., Seyed-Emami, K., & Majidifard, M. (2003). Evidence of synsedimentary tectonics in the Northern Tabas Block, East-Central Iran: The Callovian (Middle Jurassic) Sikhor Formation. *Facies, 48,* 151–170.

Fürsich, F. T., Wilmsen, M., Seyed-Emami, K., & Majidifard, M. R. (2009a). Lithostratigraphy of the Upper Triassic–Middle Jurassic Shemshak Group of Northern Iran. In M. -F. Brunet, M. Wilmsen, & J. W. Granath (Eds.), *South Caspian to central Iran Basins* (pp. 129–160). *Geological Society of London SpecialPublications*, 312. Bath: The Geological Society Publishing House.

Fürsich, F. T., Wilmsen, M., Seyed-Emami, K., & Majidifard, M. R. (2009b). The Mid-Cimmerian tectonic event (Bajocian) in the Alborz Mountains, Northern Iran: evidence of the break-up unconformity of the South Caspian Basin. In M. -F. Brunet, M. Wilmsen, & J. W. Granath (Eds.), *South Caspian to central Iran Basins* (pp. 189–203). *Geological Society of London SpecialPublications*, 312. Bath: The Geological Society Publishing House.

García-García, F., Corbí, H., Soria, J. M., & Viseras, C. (2011). Architecture analysis of a river flood-dominated delta during an overall sea-level rise (early Pliocene, SE Spain). *Sedimentary Geology, 237,* 102–113.

Geological Survey of Iran. (1995a). *Zarand, scale 1:100 000*. Tehran: Geological Survey of Iran.

Geological Survey of Iran. (1995b). *Ravar, scale 1:100 000*. Tehran: Geological Survey of Iran.

Ghasemi, A., & Talbot, C. J. (2006). A new tectonic scenario for the Sanandaj-Sirjan Zone (Iran). *Journal of Asian Earth Sciences, 26,* 683–693.

Haghipour, A., & Pelissier, G. (1977). Geology of the Saghand Sector. In A. Haghipour, N. Valeh, G. Pelissier, & M. Davoudzadeh (Eds.), *Explanatory text of the Ardekan quadrangle map* (pp. 10–68). Tehran: Geological Survey of Iran, H8.

Harms, J. C., Southard, J. B., Spearing, D. R., & Walker, R. G. (Eds.) (1975). Depositional environments as interpreted from primary sedimentary structures and stratification sequences. *Society for Sedimentary Geology (SEPM)*, *Short Course No. 2.* 164 pp.

Hashmie, A., Rostamnejad, A., Nikbakht, F., Ghorbanie, M., Rezaie, P., & Gholamalian, H. (2016). Depositional environments and sequence stratigraphy of the Bahram Formation (middle–late Devonian) in north of Kerman, south-central Iran. *Geoscience Frontiers, 7*(5), 821–834.

Horton, B. K., Hassanzadeh, J., Stockli, D. F., Axen, G. J., Gillis, R. J., Guest, B., et al. (2008). Detrital zircon provenance of Neoproterozoic to Cenozoic deposits in Iran: Implications for chronostratigraphy and collisional tectonics. *Tectonophysics, 451,* 97–122.

Huckriede, R., Ku Rsten, M., & Venzlaff, H. (1962). Zur Geologie des Gebietes zwischen Kerman und Sagand (Iran). *Geologisches Jahrbuch, vol. 51,* (pp. 197). Stuttgart: Schweizerbart Science Publishers.

Kargaranbafghi, F., Neubauer, F., & Genser, J. (2015). The tectonic evolution of western Central Iran seen through detrital white mica. *Tectonophysics, 651–652,* 138–151.

Kargaranbafghi, F., Neubauer, F., Genser, J., Faghih, A., & Kusky, T. (2012). Mesozoic to Eocene ductile deformation of western Central Iran: From Cimmerian collisional orogeny to Eocene exhumation. *Tectonophysics, 564–565,* 83–100.

Kellner, A. W. A., Dalla Vecchia, F. M., Mirzaie Ataabadi, M., De Paula Silva, H., & Khosravi, E. (2012). Review of the dinosaur record from Iran with the description of new material. *Rivista Italiana di Paleontologia e Stratigrafia, 118,* 261–275.

Leeder, M. R., & Gawthorpe, L. R. (1987). Sedimentary models for extensional tilt-block/half-graben basins. In M. P. Coward, J. F. Dewey, & P. L. Hancock (Eds.), *Continental extensional tectonics* (pp. 139–152). *GeologicalSociety of London Special Publications,* 28. Oxford: Blackwell Scientific Publications.

Leren, B. L. S., Howell, J., Enge, H., & Martinius, A. W. (2010). Controls on stratigraphic architecture in contemporaneous delta systems from the Eocene Roda Sandstone, Tremp-Graus Basin, northern Spain. *Sedimentary Geology, 229,* 9–40.

Masoodi, M., Yassaghi, A., Nogole Sadat, M. A. A., Neubauer, F., Bernroider, M., Friedl, G., et al. (2013). Cimmerian evolution of the Central Iranian basement: Evidence from metamorphic units of the Kashmar–Kerman Tectonic Zone. *Tectonophysics, 588,* 189–208.

Mattei, M., Cifelli, F., Muttoni, G., & Rashid, H. (2015). Post-Cimmerian (Jurassic–Cenozoic) paleogeography and vertical axis tectonic rotations of Central Iran and the Alborz Mountains. *Journal of Asian Earth Sciences, 102,* 92–101.

Mattei, M., Cifelli, F., Muttoni, G., Zanchi, A., Berra, F., Mossavvari, F., et al. (2012). Neogene block rotation in central Iran: Evidence from paleomagnetic data. *Geological Society of America Bulletin, 124,* 943–956.

Mattei, M., Muttoni, G., & Cifelli, F. (2014). A record of the Jurassic massive plate shift from the Garedu Formation of central Iran. *Geology, 42*(6), 555–558.

McCabe, P. J. (1987). Facies studies of coal and coal-bearing strata. In A. C. Scott (Ed.), *Coal and coal-bearing strata: recent advances* (pp. 51–66). *Geological Society of London Special Publications, 77*. Oxford: Blackwell Scientific Publications.

Miall, A. D. (1985). Architectural-element analysis: A new method of facies analysis applied to fluvial deposits. *Earth-Science Reviews, 22,* 261–308.

Miall, A. D. (2006). *The geology of fluvial deposits, sedimentary facies, basin analysis, and petroleum geology* (4th ed., p. 582). Berlin: Springer.

Morsilli, M., & Pomar, L. (2012). Internal waves vs. surface storm waves: a review on the origin of hummocky cross-stratification. *Terra Nova, 24,* 273–282.

Muttoni, G., Mattei, M., Balini, M., Zanchi, A., Gaetani, M., & Berra, F. (2009a). The drift history of Iran from the Ordovician to the Triassic. In M. -F. Brunet, M. Wilmsen, & J. W. Granath (Eds.), *South Caspian to central Iran Basins* (pp. 7–29). *Geological Society of London Special Publications*, 312, Bath: The Geological Society Publishing House.

Muttoni, G., Gaetani, M., Kent, D. V., Sciunnach, D., Angiolini, L., Berra, F., Garzanti, E., Mattei, M., & Zanchi, A. (2009b). Opening of the Neo-Tethys ocean and the Pangea B to Pangea A transformation during the Permian. *GeoArabia, 14,* 17–48.

Myrow, P. M., & Southard, J. B. (1996). Tempestite deposition. *Journal of Sedimentary Research, 66,* 875–887.

Ogg, J. G., & Hinnov, L. A. (2012). Jurassic. In F. M. Gradstein, J. G. Ogg, M. Schmitz, & G. M. Ogg (Eds.), *The geologic time scale 2012* (Vol. 2, pp. 731–791). Amsterdam: Elsevier.

Reineck, H. E., & Singh, I. B. (1973). *Depositional sedimentary environments* (p. 439). Heidelberg: Springer.

Salehi, M. A., Moussavi-Harami, S. R., Mahboubi, A., & Rahimi, B. (2014a). Palaeoenvironment and basin architecture of the Lower Jurassic Ab-Haji Formation, east-central Iran. *Boletín del Instituto de Fisiografía y Geología, 84,* 29–44.

Salehi, M. A., Moussavi-Harami, S. R., Mahboubi, A., Wilmsen, M., & Heubeck, C. (2014b). Tectonic and paleogeographic implications of compositional variations within the siliciclastic Ab-Haji Formation (Lower Jurassic, east Central Iran). *Neues Jahrbuch für Geologie und Paläontologie Abhandlungen, 271,* 21–48.

Sdzuy, K., & Monninger, W. (1985). Neue Modelle des "Jakobstabes". *Neues Jahrbuch für Geologie und Paläontologie - Monatshefte, 1985,* 300–320. Stuttgart: Schweizerbart Science Publishers.

Sengör, A. M. C. (1984). The Cimmeride orogenic system and the tectonics of Eurasia. *Geological Society of America Special Papers, 195,* 1–82.

Sengör, A. M. C., Altiner, D., Cin, A., Ustaomer, T., & Hsu, K. J. (1988). Origin and assembly of the Tethyside orogenic collage at the expense of Gondwana Land. In M. G. Audley-Charles, & A. Hallam (Eds.), *Gondwana and Tethys* (pp. 119–181). *Geological Society of London Special Publications*, 37. Oxford: Oxford University Press.

Seyed-Emami, K. (1971). The Jurassic Badamu Formation in the Kerman region, with some remarks on the Jurassic stratigraphy of Iran. *Geological Survey of Iran Report,* 19.

Seyed-Emami, K. (2003). Triassic in Iran. *Facies, 48,* 91–106.

Seyed-Emami, K., Fürsich, F. T., & Wilmsen, M. (2004a). Documentation and significance of tectonic events in the Northern Tabas block (East-Central Iran) during the Middle and Late Jurassic. *Rivista Italiana di Paleontologia e Stratigrafia, 110,* 163–171.

Seyed-Emami, K., Fürsich, F. T., Wilmsen, M., Schairer, G., & Majidifard, M. R. (2004b). Jurassic (Toarcian to Bajocian) ammonites from the Lut Block, east-central Iran. *Acta Geologica Polonica, 54*(1), 77–94.

Seyed-Emami, K., Schairer, G., Aghanabati, S. A., & Hajmolaali, A. (1993). Ammoniten aus der Badamu-Formation (oberes Toarc bis unteres Bajoc) SW von Ravar (N Kerman, Zentraliran). *Mitteilungen der Bayerischen Staatssammlung für Paläontologie und Historische Geologie, 33,* 13–30.

Seyed-Emami, K., Schairer, G., Fürsich, F. T., Wilmsen, M., & Majidifard, M. R. (2000). First record of ammonites from the Badamu Formation at the Shotori Mountains (Central Iran). *Eclogae Geologicae Helvetiae, 93,* 257–263.

Shadan, M., & Hosseini-Barzi, M. (2013). Petrography and geochemistry of the Ab-e-Haji Formation in Central Iran: implications for provenance and tectonic setting in the southern part of Tabas block. *Revista Mexicana de Ciencias Geológicas, 30,* 80–95.

Shahidi, A., Barrier, E., Brunet, M.-F., & Saidi, A. (2010). Tectonic evolution of the Alborz in Mesozoic and Cenozoic. *Geoscience Journal (in Persian), 81,* 201–216.

Shahidi, A., Barrier, E., Brunet, M. -F., Saidi, A., & Muller, C. (2007). Tectonic evolution of Alborz since Mesozoic (Iran). In Europian Geological Union (EGU) Conference, vol. 9, pp. 11074.

Sinclair, H. D. (1997). Flysch to molasse transition in peripheral foreland basins: the role of the passive margin versus slab breakoff. *Geology, 25,* 1123–1126.

Soffel, H., Davoudzadeh, M., Rolf, C., & Schmidt, S. (1996). New palaeomagnetic data from Central Iran and a Triassic palaeoreconstruction. *Geologische Rundschau, 85,* 293–302.

Soffel, H., & Förster, H. (1984). Polar wander path of the Central East Iran microplate including new results. *Neues Jahrbuch für Geologie und Paläontologie Abhandlungen, 168,* 165–172.

Stampfli, G. M., & Borel, G. D. (2002). A plate tectonic model for the Paleozoic and Mesozoic constrained by dynamic plate boundaries and restored synthetic oceanic isochrons. *Earth and Planetary Science Letters, 196,* 17–33.

Stöcklin, J. (1974). Possible ancient continental margins in Iran. In C. A. Burke & C. L. Drake (Eds.), *The geology of continental margins* (pp. 873–887). New York: Springer.

Stöcklin, J., & Nabavi, M. H. (1971). Explanatory text of the Boshruyeh Quadrangle Map 1:250,000. In Geological Survey of Iran, Report No. 3, pp. 1–50.

Takin, M. (1972). Iranian geology and continental drift in the Middle East. *Nature, 235,* 147–150.

Thierry, J. (2000). Late Sinemurian (193–191 Ma). In J. Dercourt, M. Gaetani, B. Vrielynck, E. Barrier, B. Biju-Duval, M.-F. Brunet, J. Cadet, S. Crasquin, & M. Sandulescu (Eds.), *Atlas Peri-Tethys palaeogeographical maps* (pp. 49–59). Paris: CCGM/CGMW.

Veiga, G. D., Spalletti, L. A., & Flint, S. (2002). Aeolian/fluvial interactions and high-resolution sequence stratigraphy of a non-marine lowstand wedge: the Avile Member of the Agrio Formation (Lower Cretaceous), central Neuquen Basin, Argentina. *Sedimentology, 49,* 1001–1019.

Wilmsen, M., Fürsich, F. T., & Majidifard, M. R. (2015). An overview of the Cretaceous stratigraphy and facies development of the Yazd Block, western Central Iran. *Journal of Asian Earth Sciences, 102,* 73–91.

Wilmsen, M., Fürsich, F. T., & Seyed-Emami, K. (2003). Revised lithostratigraphy of the Middle and Upper Jurassic Magu Group of the northern Tabas Block, east-central Iran. *Newsletters on Stratigraphy, 39,* 143–156.

Wilmsen, M., Fürsich, F. T., Seyed-Emami, K., & Majidifard, M. R. (2009a). An overview of the stratigraphy and facies development of the Jurassic System on the Tabas Block, east-central Iran. In M. -F. Brunet, M. Wilmsen, & J. W. Granath (Eds.), *South Caspian to central Iran Basins* (pp. 323–343). *Geological Society ofLondon Special Publications,* 312. Bath: The Geological Society Publishing House.

Wilmsen, M., Fürsich, F. T., Seyed-Emami, K., Majidifard, M. R., & Taheri, J. (2009b). The Cimmerian Orogeny in northern Iran: tectono-stratigraphic evidence from the foreland. *Terra Nova, 21,* 211–218.

Wilmsen, M., Fürsich, F., Seyed-Emami, K., Majidifard, M., & Zamani-Pedram, M. (2010). Facies analysis of a large-scale Jurassic shelf-lagoon: the Kamar-e-Mehdi Formation of east-central Iran. *Facies, 56,* 59–87.

Wilmsen, M., Fürsich, F. T., & Taheri, J. (2009c). The Shemshak Group (Lower–Middle Jurassic) of the Binalud Mountains, NE Iran: stratigraphy, depositional environments and geodynamic implications. In M. -F. Brunet, M. Wilmsen, & J. W. Granath (Eds.), *South Caspian to central Iran Basins* (pp. 175–188). *Geological Society ofLondon Special Publications,* 312. Bath: The Geological Society Publishing House.

Wright, L. D. (1985). River deltas. In R. A. Davies (Ed.), *Coastal sedimentary environments* (pp. 1–76). New York: Springer.

Zamani-Pedram, M. (2011). Source, facies, and sedimentary environments of the Middle to Upper Jurassic strata in the Kerman and Tabas areas, east-central Iran. Dissertation, *Julius-Maximilians-Universität Würzburg*, 212 pp.

Zanchetta, S., Berra, F., Zanchi, A., Bergomi, M., Caridroit, M., Nicora, A., et al. (2013). The record of the Late Palaeozoic active margin of the Palaeotethys in NE Iran: Constraints on the Cimmerian orogeny. *Gondwana Research, 24,* 1237–1266.

Zanchi, A., Zanchetta, S., Balini, M., & Ghassemi, M. R. (2016). Oblique convergence during the Cimmerian collision: Evidence from the Triassic Aghdarband Basin, NE Iran. *Gondwana Research, 38,* 149–170.

Zanchi, A., Zanchetta, S., Berra, F., Mattei, M., Garzanti, E., Molyneux, S., Nawab, A., & Sabouri, J. (2009a). The Eo-Cimmerian (Late? Triassic) orogeny in North Iran. In M. -F. Brunet, M. Wilmsen, & J. W. Granath (Eds.), *South Caspian to central Iran Basins* (pp. 31–55). *Geological Society of London Special Publications,* 312. Bath: The Geological Society Publishing House.

Zanchi, A., Zanchetta, S., Garzanti, E., Balini, M., Berra, F., Mattei, M., & Muttoni, G. (2009b). The Cimmerian evolution of the Nakhlak–Anarak area, Central Iran, and its bearing for the reconstruction of the history of the Eurasian margin. In M. -F. Brunet, M. Wilmsen, & J. W. Granath (Eds.), *South Caspian to central Iran Basins* (pp. 261–286). *Geological Society of London Special Publications, 312*, Bath: The Geological Society Publishing House.